The Palaeo-Asian ocean in the Neoproterozoic and early Palaeozoic: new geochronologic data and palaeotectonic reconstructions

E.V. Khain [a], E.V. Bibikova [b], E.B. Salnikova [c], A. Kröner [d,*], A.S. Gibsher [e],
A.N. Didenko [f], K.E. Degtyarev [a], A.A. Fedotova [a]

[a] *Geological Institute, Russian Academy of Sciences, 7 Pyzhevski per., 119017 Moscow, Russia*
[b] *Vernadsky Institute of Geochemistry and Analytical Chemistry, Russian Academy of Sciences, ul. Kosygina 19, 119991 Moscow, Russia*
[c] *Institute of Precambrian Geology and Geochronology, Russian Academy of Sciences, 2 Naberezhnaya Makarova,*
199034 St. Petersburg, Russia
[d] *Institut für Geowissenschaften, Universität Mainz, D-55099 Mainz, Germany*
[e] *United Institute of Geology, Geophysics and Mineralogy, Siberian Branch, Russian Academy of Sciences, 3 Prospekt Koptuga.,*
630090 Novosibirsk, Russia
[f] *Schmidt United Institute of Physics of the Earth, Russian Academy of Sciences, 10 Bolshaya Gruzinskaya ul., 123810 Moscow, Russia*

Abstract

The Central Asian fold belt (Urals–Mongolian belt in the Russian literature), which incorporates rock units derived from a variety of geodynamic settings, evolved the Palaeo-Asian Ocean (PAO) in the Neoproterozoic and Palaeozoic. We present new geological and isotopic data for ophiolites and metamorphic complexes of the Eastern Sayan Range of southern Siberia (Dunzhugur complex), the Polar Urals (Enganepe Range), and the Dariv and Khantaishir Ranges of western Mongolia. We also review existing geological, geochronological and palaeomagnetic data for rock assemblages indicative of past tectonic settings within that ocean. Based on these data, we suggest geodynamic reconstructions for the principal time-slices that reflect turning points in the history of this ocean at ∼1000–650, ∼650–510, and 510–450 Ma.

The age of the Circum-Siberian ophiolites is critical to constrain the timing of break-up of the large Mesoproterozoic Eurasian continent into Baltica and Siberia, and this break-up could not have occurred later than about 1100 Ma. The main events in the formation of volcanic arcs and marginal basins in the PAO were at 1000–1010, 830, 740–700, 670–640, 570, 540, and 500–490 Ma, whereas the main phases of accretion and ridge collision in the PAO were at around 800, 570, and 470 Ma. We also reconstruct the spatial positions of palaeobasins and continents at about 740 and 640 Ma.

1. Introduction

A wealth of new geologic and radiometric data has become available in recent years, suggesting the existence, from the early Neoproterozoic to the middle Palaeozoic, of a large ocean between the Mesoprotero-

* Corresponding author. Tel.: +49-6131-392163;
fax: +49-6131-394769.
E-mail addresses: Khain@geo.tv-sign.ru (E.V. Khain),
kroener@mail.uni-mainz.de (A. Kröner).

zoic and older continental blocks of Baltica, Siberia, and central Asia (Tarim, Kazakhstan, North China). This ocean is generally known in the Russian literature as the Palaeo-Asian Ocean (PAO) (Zonenshain et al., 1990). This ocean, possibly of a type similar to the present-day West Pacific, closed in the late Palaeozoic after a long history of arc and microcontinent accretion to form the Central Asian fold belt (CAFB) (Mossakovskii et al., 1993), also known as the Altaids (Sengör et al., 1993) or, in the Russian literature, as the Urals–Mongolian fold belt (Muratov, 1974). Fragments of rock units formed in a variety of geodynamic settings are preserved in this belt. We elucidate the inception time of this palaeo-ocean, its main evolutionary stages, and its inferred spatial position.

Large areas of the CAFB have been covered by terrane mapping, and several palaeotectonic settings have been proposed (Khain and Bozhko, 1988; Zonenshain et al., 1990; Mossakovskii et al., 1993; Sengör et al., 1993; Sengör and Natal'in, 1996; Berzin et al., 1994).

Palaeo-reconstructions, however, are possible only for the late Neoproterozoic to Palaeozoic history of the CAFB because most of these terranes obtained their final shapes no earlier than the Ordovician.

On our proposed tectonic reconstructions, we show the outlines of rock units with reliable radiometric ages and specific geodynamic settings, as well as their location in the general framework of the PAO. We have developed new tectonic reconstructions for three principal time slices, reflecting the turning points in the history of the PAO, namely at ∼1000–650, 650–510, and 510–450 Ma.

We distinguish two parts in the structure of the CAFB (present-day reference frame): the western, Tarim–Kazakhstan (Ural, Kazakhstan, Tien Shan, Tarim northwestern China), and the eastern, Siberian–Mongolian (Taimyr, Yenisey Range, Altai–Sayan region, Transbaikalia, Mongolia). These differ in terms of structural features and tectonic evolution. This dissimilarity may be due to the intrinsic spatial

Fig. 1. Overview map of Central Asia showing location of study area and detailed maps.

separation of these parts from one another and their respective development on the Tarim–Kazakhstan and Siberian–Mongolian margins of the PAO. The difference in their origin may be illustrated by correlating events on opposite margins of the palaeo-ocean during the main stages of its development.

New radiometric data from a variety of tectonic units, including ophiolites, have been obtained for the ~1000–570 Ma time interval; reconstructions showing the position of the main continental blocks have been compiled for ~740 and 640 Ma. The position of the main continental blocks and oceanic basins is in accordance with the available palaeomagnetic data. Fig. 1 shows a map of central Asia outlining the areas from which we report data and field observations and on which our palaeoreconstructions are based.

2. New age data for ophiolites is southern Siberia, western Mongolia, and the Polar Urals

2.1. Southeastern part of Eastern Sayan (Dunzhugur ophiolite)

The Eastern Sayan mountain range is situated west of Lake Baikal, just north of the Mongolian border (Figs. 1 and 2). Ophiolites are well exposed in this part of southern Siberia and have been studied in detail in the southern part of Eastern Sayan (Dobretsov et al., 1985; Khain et al., in press). They are developed around the Gargan block (Fig. 2) that consists of Mesoproterozoic high-grade metamorphic rocks, mainly gneisses with a minimum U–Pb zircon age 2160 Ma, that were overprinted during a tectono-metamorphic event between 450 and 480 Ma ago (U–Pb zircon data; Khain et al., 1995a). Sm–Nd isotpic data confirm the ancient origin of these gneisses, and $\varepsilon_{Nd(t)}$-values between −6.4 and 8.1 and mean crustal residence ages of 1.63 and 1.81 Ga document a long crustal history. We proposed that events approximately 470 Ma followed obduction of ophiolites and may be related to ridge subduction (Khain et al., 1995b). The structural framework is defined by granite-gneiss domes, which deform tectonic sheets (nappes) composed of ophiolitic rocks and a carbonate shelf assemblage of the Khamardaban–Gargan microcontinent (Fig. 2). Northwestern and southeastern ophiolite belts are distinguished there, which stretch for about 100 km

and join at the eastern and western closures of Gargan antiform in the region of the Ospa–Kitoy Goltsy (bald peaks) (Fig. 2). The most complete ophiolite sections are exposed in the Ospa–Kitoy Goltsy and near Dunzhugur Mountain (Khain et al., in press).

In the Ospa–Kitoy Goltsy, the ophiolite is strongly disturbed tectonically, and a series of tectonic slices has been recognized. The largest consists of tectonized dunite–harzburgite and serpentinite mélange. The mélange contains blocks of dunite, harzburgite, wehrlite, pyroxenite, and gabbro along with minor dolomite. The most complete but disrupted ophiolite sequence is exposed at the eastern part of Gargan zone, which includes slabs of serpentinite after peridotite, layered gabbro, diabase dykes, and basaltic rocks. The ophiolite nappe is thrust onto the terrigenous Il'chir Schist Formation (late Neoproterozoic to early Cambrian) and is stratigraphically overlain by carbonate–shale turbidites of the Ospa Formation (late Neoproterozoic to early Cambrian). Olistostromes are present in both formations, with olistoliths made up of ophiolite fragments, dolomites and limestones of likely late Neoproterozoic (=Vendian) age.

In the valleys of the Oka and Bokson Rivers (western Gargan zone), an ophiolite association was mapped as the Dunzhugur ophiolite complex (Dobretsov et al., 1985). On the eastern side of the Oka River, upstream from the confluence with the Bokson River, Sklyarov (1988) described the following succession, from bottom to top: serpentinite after peridotite; a transitional zone of peridotite, pyroxenite and gabbro; coarse-grained layered diopside–anorthite gabbro; cumulate pyroxene–amphibole gabbro; gabbro–diabase sheeted dykes ranging in chemistry from picritic basalt to boninite and andesite; basaltic pillow lava and pillow breccia, followed by basaltic andesite and andesite. The Dunzhugur ophiolitic lavas are stratigraphically overlain, on Dunzhugur Mountain, by carbonate–shale turbidites of the Dunzhugur formation of proposed late Riphean age. The turbidite sequence contains numerous sills of high-Ti basalt and includes olistostromes and olistostrome horizons with fragments of ophiolite, dolomite and limestone. The Vendian–early Cambrian carbonate complex of the Boxon Group was thrust over the ophiolite nappe.

We have chosen pyroxenites and plagiogranites of the Dunzhugur complex for geochronology (Fig. 2).
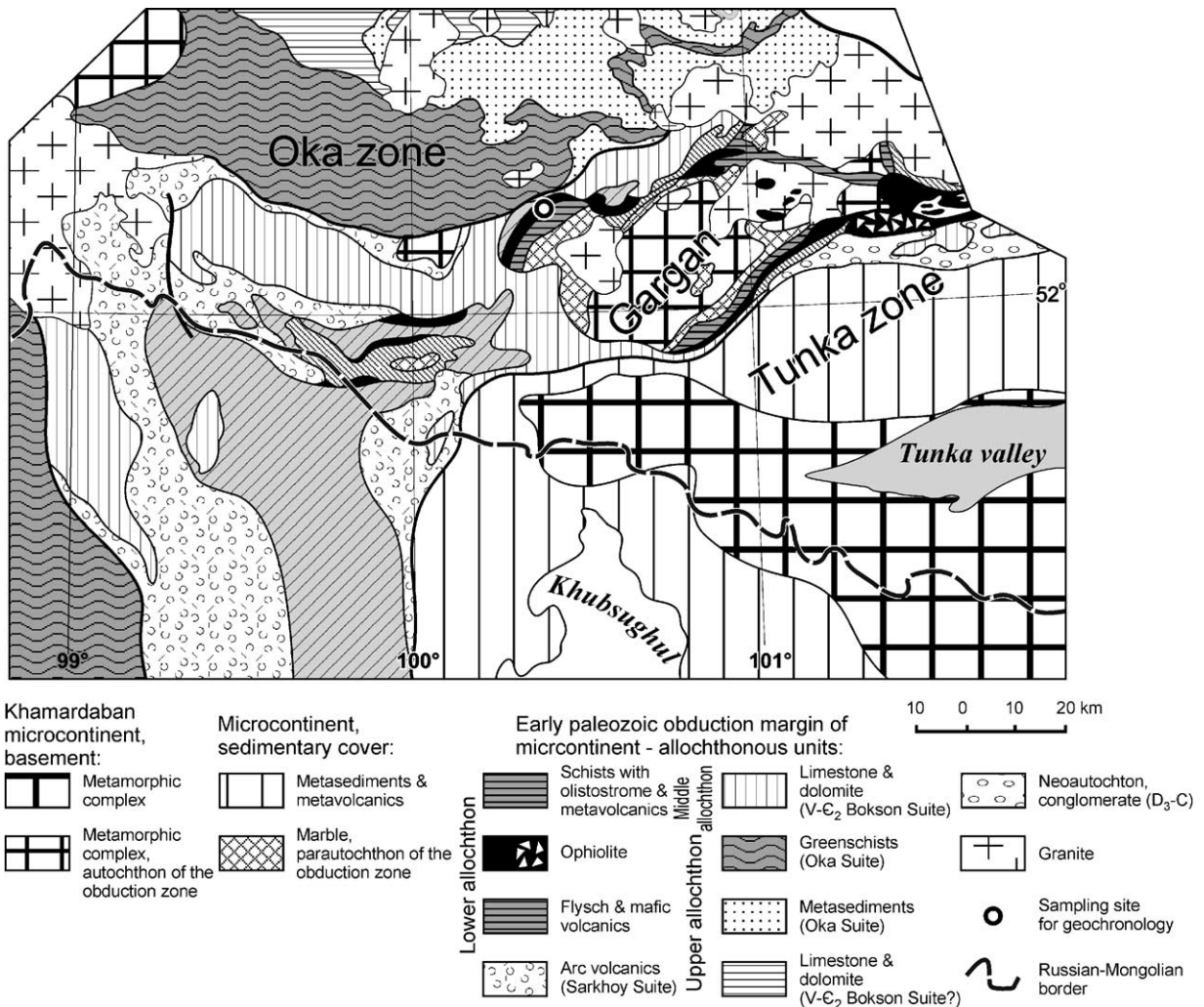
Fig. 2. Main litho-tectonic units of the southern East Sayan Range. Grey line is Russian–Mongolian border.

Pyroxenite was selected because it preserves its primary magmatic mineralogy. Clinopyroxene (Cpx) concentrates were extracted from three pyroxenite samples for Sm–Nd isotopic analysis, and three whole rock/Cpx tie-lines yielded ages between 1.7 and 1.55 Ga. The corresponding REE spectra and isotope data imply that the whole-rock and Cpx samples were not in isotopic equilibrium. The Cpx analyses alone are aligned along a poorly defined chord (MSWD $= 9.3$) with $T = 1270 \pm 110$ Ma.

Zircons from a large sample of plagiogranite from one of several isolated intrusive bodies at the boundary

between the gabbroic rocks and sheeted dykes were dated by Khain et al. (in press). Two multigrain magmatic zircon fractions, analyzed by the conventional U–Pb method, yielded a mean $^{207}Pb/^{206}Pb$ age of 1022 ± 10 Ma, whereas three fractions of 3–4 grains each were analyzed by the evaporation technique and provided a mean $^{207}Pb/^{206}Pb$ age of 1019.9 ± 0.7 Ma (Khain et al., in press). This age is interpreted to reflect the time of crystallization of the plagiogranite and formation of the ophiolite. Judging from the chemical composition of the ophiolitic rocks, they formed in a supra-subduction zone setting, and the Dunzhungur

marginal ocean basin must have begun to open prior to 1020 Ma (Khain et al., in press).

2.2. Crystallization age of the Bayannor ophiolite, Dariv Range, western Mongolia

The Eastern Sayan ophiolite belt extends southwards into northern and western Mongolia, where it is involved in the structure of the Dariv–Shishkhid–Gargan obduction zone (Khain, 1991; Gibsher et al., 1991). This belt marks the western and northern borders of the Khamardaban–Gargan and Central Mongolian microcontinents.

Until recently, most workers considered the ophiolites of this zone to be late Neoproterozoic to Cambrian in age or older (Kheraskova et al., 1985; Tomurtogoo, 1989). One of the most complete ophiolite successions is exposed in the Dariv Range in western Mongolia (Fig. 3) (Khain, 1989; Khain et al., 1995a,b). The geological map of the Dariv Range portrays two principal structural features reflecting obduction and remobilization episodes: an allochthonous ophiolitic assemblage and granite-gneiss domes that deform the ophiolite nappes (Khain, 1989). In the northeastern and central parts of the structure, the autochthonous complex is represented by volcanic and sedimentary rocks that were deposited on the margins of the central Mongolian microcontinent and display greenschist to amphibolite and locally granulite facies metamorphism (Khain et al., 1995a). Characteristic structural features of the metamorphic core of the Dariv Range are pyroxenite and gabbro
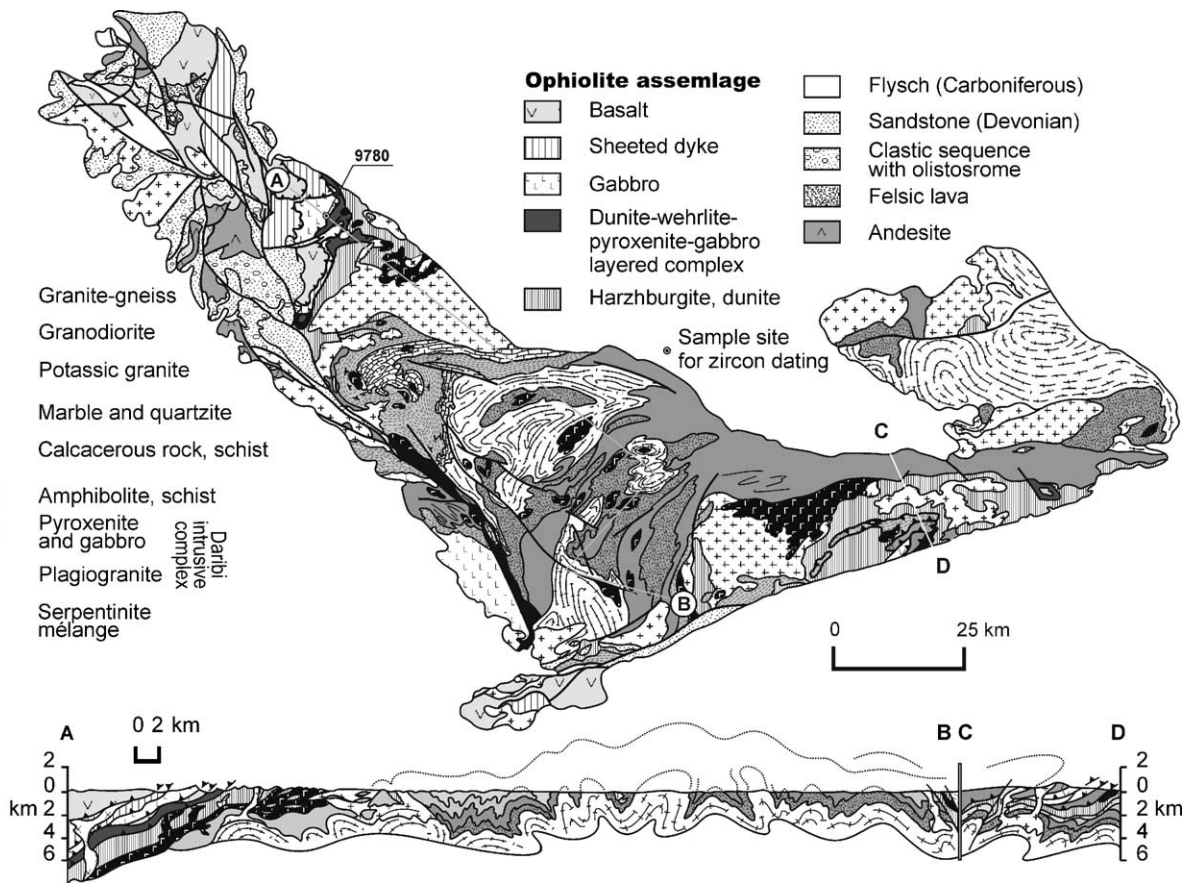

Fig. 3. Geological map of the Dariv Range, western Mongolia. Compiled by E. Khain using unpublished material of Tomurtogoo and Kheraskova. Fine white lines A–B and C–D are profiles displayed at bottom of figure.

intrusions that cut through the autochthonous rocks, intrude the lower part of the ophiolite and occur as xenoliths in the granites and granite-gneisses. Gabbro samples from a differentiated sill in the central part of the range yielded a Sm–Nd mineral isochron corresponding to an age of 457 ± 40 Ma ($\varepsilon_{Nd(t)} = -8.8$, $T_{DM} = 1.8$; Khain et al., 1995a). U–Pb data on zircons from a hypersthene-garnet granulite and a syntectonic tonalite from the central part of the range (499 ± 2.5 and 490 Ma, respectively) were also obtained (Kozakov et al., 2002).

In the northwestern part of the range, a NW-dipping thrust package (Fig. 3, sections A and B), consists of a complete ophiolitic suite, which was named the Bayannur ophiolite (Khain, 1989; Khain et al., 1995a). The base of the suite is made up of a tectonized dunite–harzburgite assemblage. In a NW direction, these rocks are overlain by dunite-pyroxenite and, farther upsection, by pyroxenite-gabbro. Gabbroic rocks of a layered cumulate sequence pass into sheeted and fractured dykes which, in turn, are overlain tectonically by a thrust slice that consists mainly of tholeiitic lavas. Farther west, the lava slice is overthrust by another slice of sheeted dykes and by a slice composed of differentiated basalt-rhyolite volcanic rocks.

We collected sample 9780 for zircon dating from a plagiogranite occurring in the upper part of the gabbroic sequence near the boundary of the dyke complex (Fig. 3). Minor plagiogranite bodies and veins have intrusive contacts with the gabbronorites of the layered series, and apophyses and small veins branch off these bodies. The analytical procedure and data are given in the Appendix A and Table 1.

Sample 9780 contains euhedral and subhedral, transparent, yellowish, homogenous zircon crystals with prismatic and short prismatic habit. The crystal size is 50–150 μm with a length/width ratio of 1.5–2.5. Three multigrain fractions, including one abraded fraction of the cleanest zircon grains, were analysed (nos. 1–3, Table 1; Fig. 4A). The data points are slightly discordant and define a regression line (MSWD = 0.14) with intercept ages at 577 ± 75 and 266 ± 355 Ma, respectively. The clustering and scatter of data points close to the concordia curve resulted in significant uncertainties in the upper intercept age. However, the weighted mean $^{207}Pb/^{206}Pb$ age of all three analysed zircon fractions is 571 ± 4 Ma, identical to the U–Pb age of 573 ± 6 Ma for the concordant

analysis of the abraded zircon fraction as well as the upper intercept age. We, therefore, consider the age of 571 ± 4 Ma to approximate the time of plagiogranite crystallization of the Bayannur ophiolite.

The above zircon data, in conjunction with previous zircon ages (Khain et al., 1995a; Kozakov et al., 2002), suggest the presence of a late Neoproterozoic, Vendian ophiolite in the Dariv Range that was obducted onto the margin of the central Mongolian microcontinent at the end of the Cambrian. The geochemical signature of the ophiolite points to a fore-arc spreading setting (Khain et al., 1995a).

2.3. Ophiolite age from the Khantaishir Range, western Mongolia

The Khantaishir ophiolite has been viewed as a fragment of the island-arc Ozernaya lithotectonic zone of western Mongolia (Dergunov, 1989) in the framework of the Central Asian fold belt. At different times it was interpreted as (i) a remnant of a Vendian to early Cambrian intra-oceanic volcanic arc, (ii) an early Cambrian primitive island arc, or (iii) Vendian to early Cambrian oceanic crust of a back-arc basin (Zonenshain and Kuzmin, 1978). Its poorly constrained age resulted from different interpretations of how the limestones of the Upper Khantaishir Formation, containing early Cambrian (Atdabanian) archaeocyatha, are related to the siliceous sediments of the Lower Khantaishir Formation, which directly overlie the ophiolitic suite. To resolve these issues, we studied the Khantaishir ophiolite suite on the southern slope of the Khantaishir Range near the beginning of the Suvra-Gol River (Fig. 5). We have reconstructed the full ophiolite section from several tectonic blocks which, from bottom to top, is:

- *Block 5*: A layered series, near an elevation of 2890 m above sea level, comprises five rhythmic units composed of dunite, wehrlite (websterite), clinopyroxenite plus websterite, and gabbronorite. The gabbronorite is cut by tonalite and plagiogranite veins (exposed width is 1250 m).
- *Block 4*: A layered series, comprising two rhythmic units with dunite, pyroxenite, and gabbronorite (150 m); massive gabbronorite (600 m) with plagiogranite veins and pillow lavas with siliceous sediments (300 m), intruded by swarms of roughly

Table 1

U–Pb isotopic data for multigrain analyses of zircons from plagiogranite samples of ophiolite complexes from the Palaeo-Asian ocean

No.	Fraction size (μm)	Weight (mg)	Concentration (ppm)		$^{206}Pb/$ ^{204}Pb[a]	Isotopic ratios corrected for blank and common Pb[b,c]				Rho[d]	Age (Ma)		
			Pb	U		$^{207}Pb/^{206}Pb$	$^{208}Pb/^{206}Pb$	$^{207}Pb/^{235}U$	$^{206}Pb/^{238}U$		$^{207}Pb/^{235}U$	$^{206}Pb/^{238}U$	$^{207}Pb/^{206}Pb$
Dariv Range, western Mongolia													
(1) 9780	+85–100	0.15	18.2	177	440	0.0590 ± 4	0.1671	0.7250 ± 53	0.0892 ± 4	0.53	554 ± 4	551 ± 2	566 ± 13
(2) 9780	+60–85	0.68	19.9	195	706	0.0591 ± 1	0.1616	0.7396 ± 30	0.0907 ± 3	0.87	562 ± 2	560 ± 2	571 ± 4
(3) 9780	+85–100 30%[a]	1.10	6.28	61.4	779	0.0592 ± 2	0.1711	0.7507 ± 32	0.0920 ± 3	0.75	569 ± 2	567 ± 2	573 ± 6
Khantaishir Range, western Mongolia													
(4) 9760	+60–75	0.36	16.1	149	639	0.0590 ± 2	0.3201	0.7021 ± 28	0.0862 ± 3	0.76	540 ± 2	533 ± 2	569 ± 6
(5) 9760	>75	0.48	18.5	173	884	0.0590 ± 2	0.3160	0.7075 ± 30	0.0870 ± 3	0.74	543 ± 2	538 ± 2	567 ± 6
(6) 9760	>75 40%[a]	0.49	9.12	56.9	115	0.0590 ± 4	0.3585	0.7240 ± 54	0.0889 ± 3	0.50	553 ± 4	549 ± 2	569 ± 14
Enganepe Range, Polar Urals													
(7) 2114	+90	2.1	23.31	177	425	0.0959 ± 19	0.2302	0.9528 ± 80	0.1114 ± 3	0.58	680 ± 8	681 ± 4	674 ± 37
(8) 2114	−90 + 60	1.0	31.51	288	2900	0.0666 ± 2	0.1110	0.9321 ± 30	0.1097 ± 3	0.70	669 ± 2	670 ± 4	662 ± 6
(9) 2114	−60	1.6	14.58	137	1800	0.0698 ± 2	0.1144	0.9003 ± 40	0.1056 ± 3	0.58	652 ± 2	647 ± 3	668 ± 9

All errors are 2σ.

[a] Percentage of zircon removed during air-abrasion.

[b] Measured ratio.

[c] Uncertainty (95% confidence level) refers to last digit of corresponding ratio.

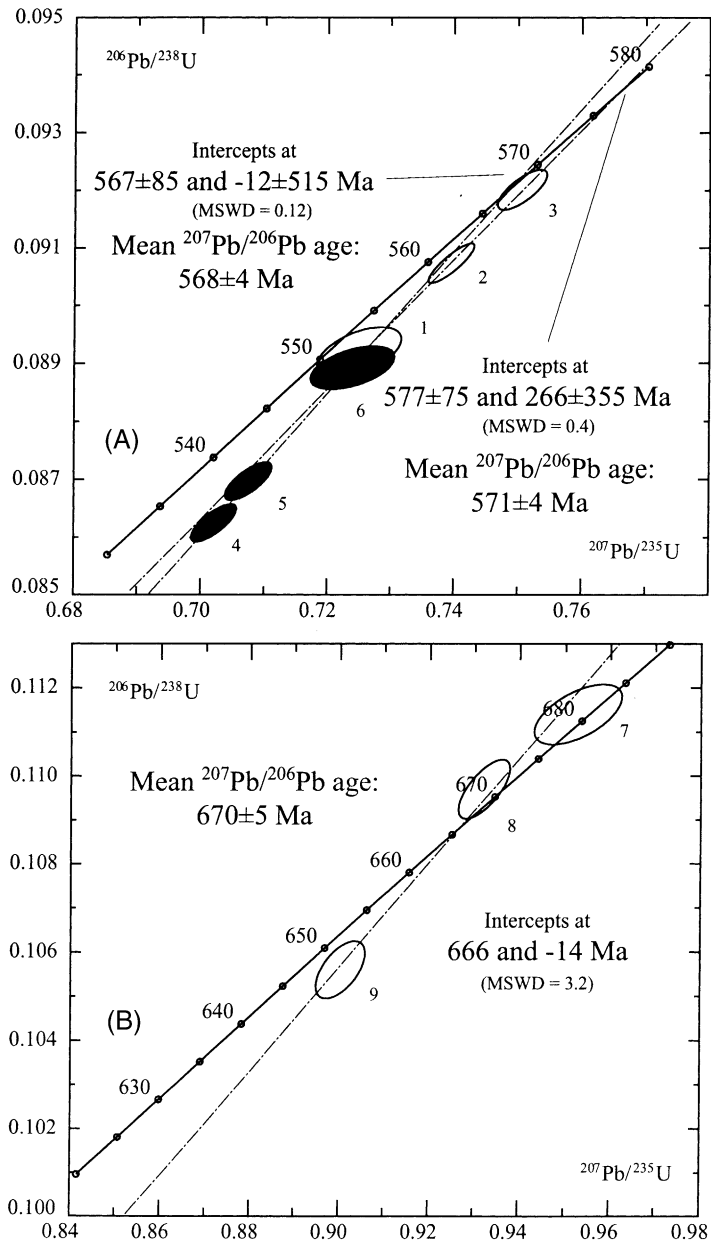[d] Correlation coefficient of $^{207}Pb/^{235}U$ vs. $^{206}Pb/^{238}U$.

Fig. 4. Concordia diagrams showing U–Pb data for multigrain zircon fractions from plagiogranites of (A) Dariv (open ellipses) and Khantaishir (full ellipses), and (B) Enganepe Ranges. For analytical data, see Table 1.

parallel mafic dykes that, jointly with the gabbronorite, are cut by dolerite sills (400 m) and a package of mafic sheeted dykes and half-dykes (ca. 350 m). Some of the dykes may be feeders to diopside basalt sills.

- *Block 3*: Dolerite sills (incompletely exposed width of 750 m) and differentiated gabbros are intrusive into earlier sills and are cut themselves by a younger generation of dykes; pillow lavas (1200 m) are intruded almost conformably by dolerite sills. Banded
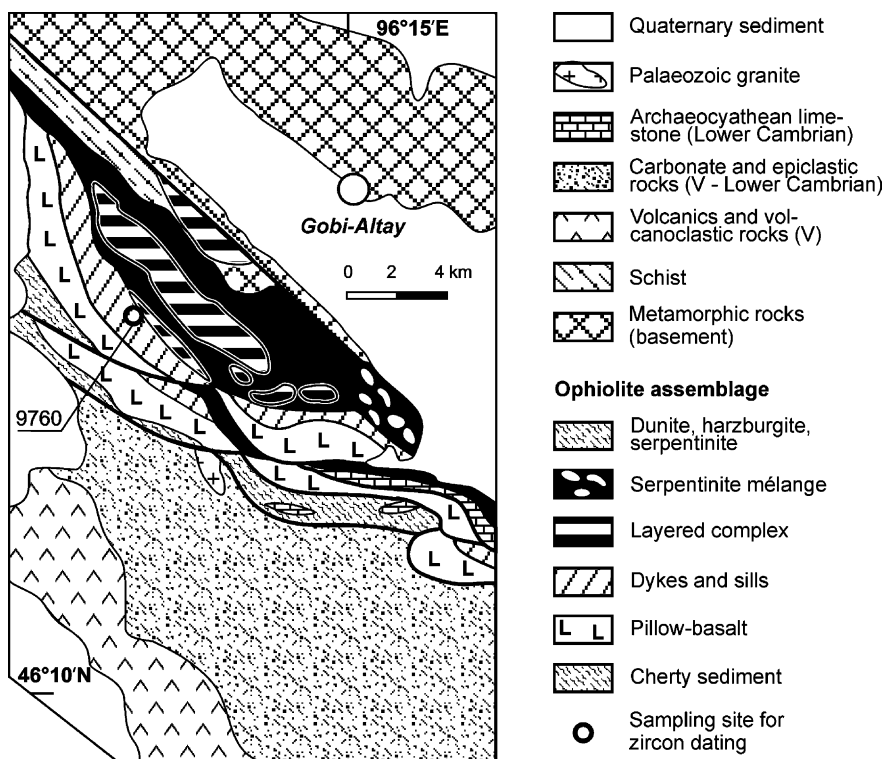
Fig. 5. Geological map of Khantaishir Range, western Mongolia. Compiled by Gibsher and Khain, using material of Zonenshain and Kuzmin (1978).

purple and green cherts and mud-silt distal turbidites (250 m) overlie pillow lavas and contain sporadic beds of debris flow sediments and are overlain, in Block 1, by flysch sediments of the Naran Formation. The exposed outcrop width of ophiolite and overlying sediments exceeds 4000 m.

- *Blocks 2 and 1*: Pillow lavas are interlayered with chert and clastic sediments (for further details, see Gibsher et al., 2001)

We selected plagiogranite sample M 9760 from Block 4 for zircon dating (for location, see Fig. 5). The plagiogranite is confined to the margin of an isotropic gabbronorite massif near its contact with the layered series. Plagiogranite makes up vein-like bodies, 1–50 cm wide, piercing the gabbronorites along a system of variably oriented joints. The plagiogranite, in turn, is cut by mafic dykes trending NE and likely related to the sheeted dykes in Block 4. No plagiogranites have been detected in the dyke or sill

suites. According to Zonenshain and Kuzmin (1978, unpublished data), the plagiogranites are very low in K_2O (0.4%), Rb (2.3 ppm), Ba (110 ppm), and Sr (110 ppm) and display geochemical fingerprints of oceanic plagiogranites.

Zircons from plagiogranite sample 9760 are yellowish pink, translucent or somewhat turbid, subhedral, or euhedral and prismatic. Turbid crystals often have resorbed prism faces (1 0 0) and contain irregularly shaped metamict domains (relic cores?) traced by numerous mineral inclusions. Transparent and translucent zircon crystals are homogeneous and contain minute mineral and bubble-like inclusions. The crystals are 40–150 μm in size with length/width ratios of 1.5–2.5.

Two unabraded and one abraded (whereby 40% of zircon material was removed) multigrain fractions of transparent and translucent zircons (nos. 4–6, Table 1) were analyzed. The data points define a regression line (MSWD = 0.1) with concordia intercept ages at

568 ± 86 Ma and -10 ± 514 Ma (Fig. 4A). The large error in the upper intercept age, just as in the Dariv plagiogranite sample, is due to data points clustering tightly near the upper discordia intercept. The mean $^{207}Pb/^{206}Pb$ age of all four zircon analyses is 568 ± 4 Ma and is identical to the upper concordia intercept age. This is interpreted as the best estimate for the time of plagiogranite crystallization and formation of the Khantaishir Range ophiolite.

From the above age, and the geochemical data of Zonenshain and Kuzmin (1978), we conclude that the Khantaishir ophiolite formed in latest Neoproterozoic time, most likely in a fore-arc basin in a supra-subduction zone setting.

2.4. Ophiolite age from the Enganepe Range, Polar Urals

Neoproterozoic ophiolites also occur in the northwestern part of the Central Asian fold belt in the Polar Urals (Fig. 6), where pre-Ordovician and pre-latest Neoproterozoic units occupy the lowest tectono-stratigraphic position and are structurally discordant with respect to the typical NE trend of the Urals orogenic belt. The most spectacular example of these relationships occurs in the Enganepe Range, on the eastern slope of the Polar Urals (Fig. 6), where faunally-dated late Cambrian to Ordovician strata overlie strongly dismembered NW-striking older units. The Kharbei and Kharmatolous metamorphic complexes, exposed beneath giant Palaeozoic ophiolitic nappes, are also considered to be pre-Ordovician in age (Fig. 6A). The ages of these rocks, however, remain uncertain, and we therefore dated zircons from a plagiogranite from the Enganape Range (Fig. 6B).

The Enganepe Range is unique in the entire Urals because strongly deformed flysch, volcano–sedimentary, and volcanic assemblages including fragments of an ophiolite are exposed below slightly deformed late Cambrian to early Ordovician strata (Dushin, 1997). There is a sharp structural, metamorphic, and stratigraphic break at the contact with the early Palaeozoic rocks. Numerous pebbles of serpentinite and mafic volcanic rocks occur in the Cambrian–Ordovician basal conglomerate (Dushin, 1997).

Several nappes inclined to the northeast and cut by subvertical NW–SE trending faults can be distinguished in the pre-Palaeozoic, northern Enganepe Range. According to Dushin (1997), this range incorporates the Manyukuyuakha tectonic zone, where ophiolite outcrops are widespread (Fig. 6B). This zone is considered to be part of a large NW-striking fault zone, which extends for more than 70 km outside the Enganepe Range (Fig. 6A). Along its entire length, lens-shaped meta-ultramafic bodies (Enganepe Complex) measure tens to hundreds of meters wide by several kilometers long.

One of the largest serpentinite mélange outcrops is found in the gorge of the Yanas-Keu-Lek-Tal'ba Creek, a right tributary of the Bolshaya Usa River (Fig. 6B). Its exposed width is about 300 m, and it can be traced along strike for 5 km. The mélange matrix is composed of strongly tectonized chrysotile-lizardite serpentinite. Blocks in the mélange range from a few tens of centimetres to several tens of metres in size, the largest blocks reaching 50 m. Of several large blocks on the left bank of the Yanas-Keu-Lek-Tal'ba Creek, one is composed of ophicalcite, the product of carbonatization resulting from underwater erosion of ultramafic rocks. Carbonatized dunites and harzburgites occur as clastic fragments in the ophicalcite, and fragments of the metamorphic structure of the dunite–harzburgite complex (mineral lineations and compositional layering) can be recognized on weathered surfaces, suggesting the presence of mantle tectonites. Gabbros make up several blocks in the mélange. A large block som 50–60 m in diameter contains gabbro-amphibolite, amphibolized quartz diorite, plagiogranite, as well as brecciated diabase dykes and sills (1.5–2 m wide). We collected sample 2114 from the plagiogranites for zircon dating and Sm–Nd isotopic analysis (Fig. 6B).

The gabbro-amphibolites and plagiogranites are composed of blue-green, long-prismatic amphibole crystals (ca. 30%), tabular plagioclase crystals replaced by saussurite or an aggregate of epidote, zoisite, sericite, and quartz. Granulated quartz appears in the quartz diorites. The rocks show a relict subhedral granular texture. Secondary chlorite-quartz aggregates are elongated along the foliation. In the plagiogranite, the main minerals are quartz and plagioclase (slightly to completely replaced by epidote, chlorite and sericite). Accessory minerals are sphene, zircon, and apatite. In sample 2114, zircon is represented as well-formed crystals of predominantly
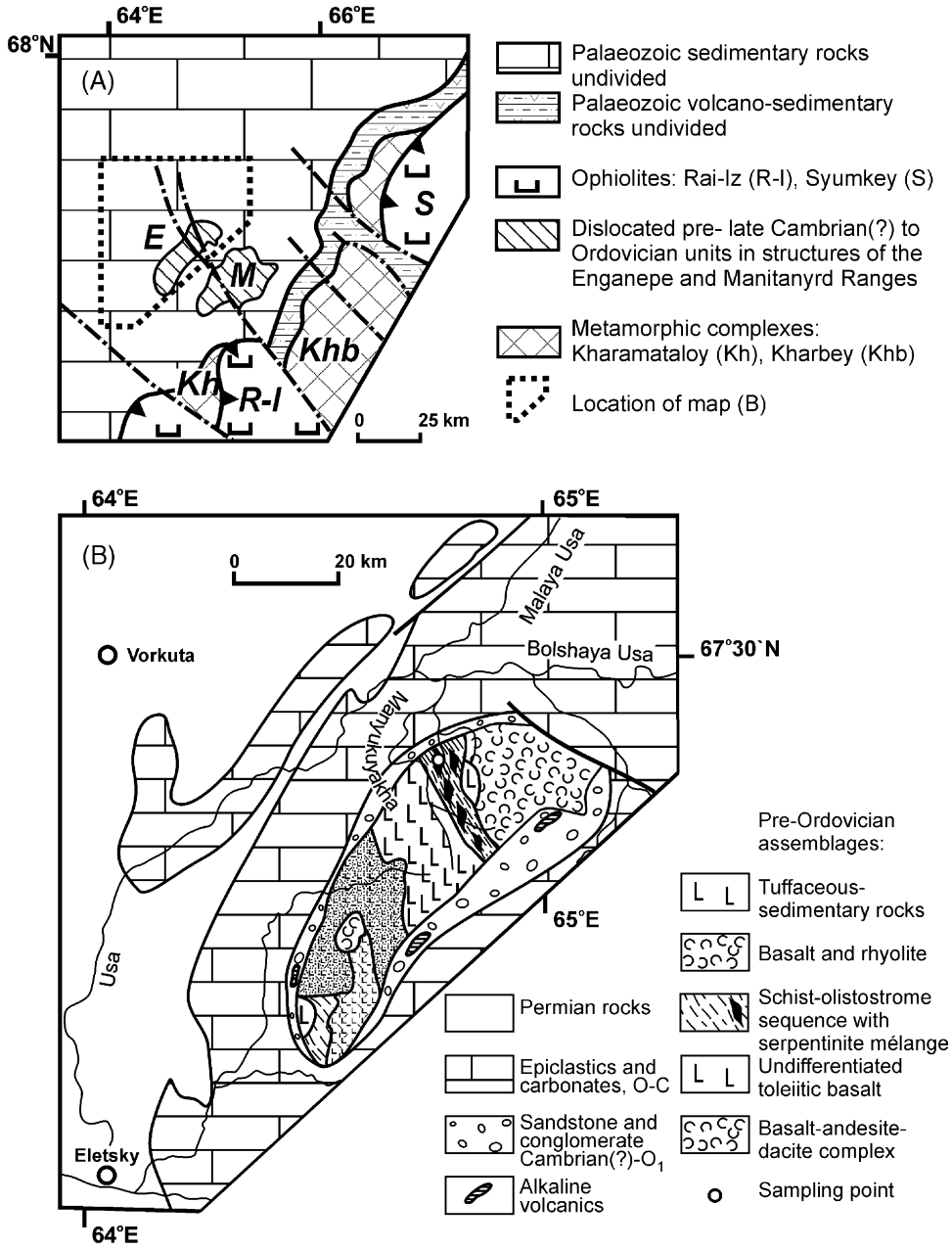
Fig. 6. Principal litho-tectonic units of the Polar Urals (A) and simplified geological map of the Enganepe Range (B), modified after Dushin (1997).

hyacinth habit. They are transparent, light-brown, and many grains are fractured. The zircon morphology suggests a magmatic origin. The analytical procedures and data are given in the Appendix A and in Table 1.

The zircons are low in uranium, which is in accordance with their genesis in a U-poor environment such as a magma chamber below a mid-ocean ridge. Concordant ages were obtained for two coarse zircon

Table 2
Sm–Nd isotopic data and REE analyses (in ppm) for plagiogranite sample 2114 from Enganepe Range, Polar Urals

Sm	Nd	$^{147}Sm/^{144}Nd$	$^{143}Nd/^{144}Nd$	ε_{Nd} (670 Ma)	T_{DM} (Ga)	La	Ce	Nd	Sm	Eu	Gd	Dy	Er	Yb
0.941	3.68	0.1547	0.512540 ± 7	+1.7	1.57	3.29	7.54	3.91	1.01	0.34	1.16	1.34	0.90	0.99

Analyses were performed at the Institute of Geology of Ore Deposits, Russian Academy of Sciences, Moscow by D.Z. Zhuravlev, using a Finnigan-MAT 262 mass spectrometer. Analytical details are given in Zhuravlev et al., 1987. Result for La Jolla: $^{143}Nd/^{144}Nd = 0.511840 \pm 15$ ($n = 25$, 2σ error of the population). Concentrations in ppm; error is 1% relative. Error in $^{143}Sm/^{144}Nd$ is 0.2% relative.

fractions within the limits of experimental error (Fig. 4B). The small zircon fraction shows some loss of radiogenic Pb. However, its $^{207}Pb/^{206}Pb$ age equals the age obtained for the two concordant fractions. Based on these results, the combined mean zircon age for the plagiogranite is 670 ± 5 Ma (Khain et al., 1998). The whole-rock plagiogranite sample 2114 was also studied by the Sm–Nd method. For an age of 670 Ma, the $\varepsilon_{Nd(t)}$-value is +1.7 and the corresponding Nd model age is 1.6 Ga (Table 2). The Nd isotopic data suggest some involvement of older continental material in the generation of the plagiogranite magma, perhaps subducted sediment. The REE pattern, based on isotope dilution analysis (Table 2), also suggests that the plagiogranite sample belongs to the ophiolite.

Dushin (1997) showed that the mélange blocks occur within a sedimentary sequence comprising strongly schistose sandstones and siltstones, full of tectonic blocks and lenses of volcanic and sedimentary material. The most complete sequence is exposed along the Manyukuyakha River. It comprises schistose siltstones and graded sandstones, numerous blocks of serpentinite, tectonized volcaniclastic sandstone, and conglomerate. It is unlikely that all these rocks originally constituted a continuous sedimentary sequence, but due to poor exposure their original relationships cannot be verified. We interpret these rocks as constituting a deep water sequence with olistostrome horizons or numerous tectonic lenses and wedges. Dislocated blocks of the disintegrated ophiolite occur widely as olistoliths or tectonic lenses in this sequence.

In the west, the sedimentary sequence occurs at high-angle tectonic contact with poorly differentiated tholeiitic basalts (Fig. 6B). In the east, it is overridden by a nappe consisting of volcanogenic-sedimentary rocks. At the base of the nappe, aphyric basalt altered to greenschist and overlain by a pillow lava horizon is injected by diabase dykes and sills (Dushin, 1997).

The pillows contain a 2-m thick horizon of argillite and siltstones. The outcrop width of the volcanic rocks is about 800 m. A schist-volcanogenic unit (200 m thick), composed of interlayered aphyric and sparsely porphyric basaltic flows with dark grey sandstones, shales and jaspers makes up the upper part of sequence. Sediments constitute no more than 10–15% of the entire unit, and boninites occur in tectonic lenses.

In summary, we have identified a series of thrust sheets in the northern Enganepe Range, brought together prior to the late Cambrian. These sheets contain rocks derived from island arcs and their slopes (Dushin, 1997). Based on new geochemical data, there are tholeiitic, arc tholeiitic, and OIB-like basalts and adakites in the volcanogenic thrust sheet (Scarrow et al., 2001). These authors also suggested a supra-subduction zone origin and speculated on an arc-forearc tectonic setting for the complex. Forearc basin relicts now compose blocks in the mélange, and the presence of ophicalcites points to submarine (basin floor) weathering of ultramafic rocks. Our zircon age shows that all these ophiolitic rocks already existed in the late Neoproterozoic.

3. Proposed evolution of the Palaeo-Asian ocean during the interval ~1100–450 Ma

3.1. Terminal Mesoproterozoic to late Neoproterozoic (~1100–650 Ma)

Crystalline basement complexes in the microcontinents in western Kazakhstan part (present reference frame) are known as Kokchetav, Ulutau, Tarim and others (Figs. 7 and 8). Metamorphism and granite formation were dated at 1800–1900 Ma (Khalilov et al., 1993), and this suggests the existence, in Mesoproterozoic time, of a continuous Kazakhstan–Tarim block with continental crust of the above age. This block

probably broke up into several separate crustal fragments in the Neoproterozoic to early Palaeozoic.

Epicontinental basins and passive margins of the Siberia and Tarim–Kazakhstan continents can be reconstructed as from about 1100 Ma ago (see also Pisarevski and Natapov, in press; Figs. 7 and 8). Along the Siberian margin, carbonate-clastic assemblages overlie pre-Riphean (>1600 Ma) rocks with erosional unconformities. This is best demonstrated in the Patom–Bodaibo zone in Transbaikalia (east of Lake Baikal), where clastic sediments with carbonates and carbonaceous schists, mafic volcanics, volcano–sedimentary rocks and quartz sandstones, dolomite, and limestone are dominant (Balaganakh Formation). The facies succession reflects the following settings: shelf—continental slope—continental rise, with sedimentary input into the basin (Sovetov and Blagovidov, 1995). Similar sequences are found
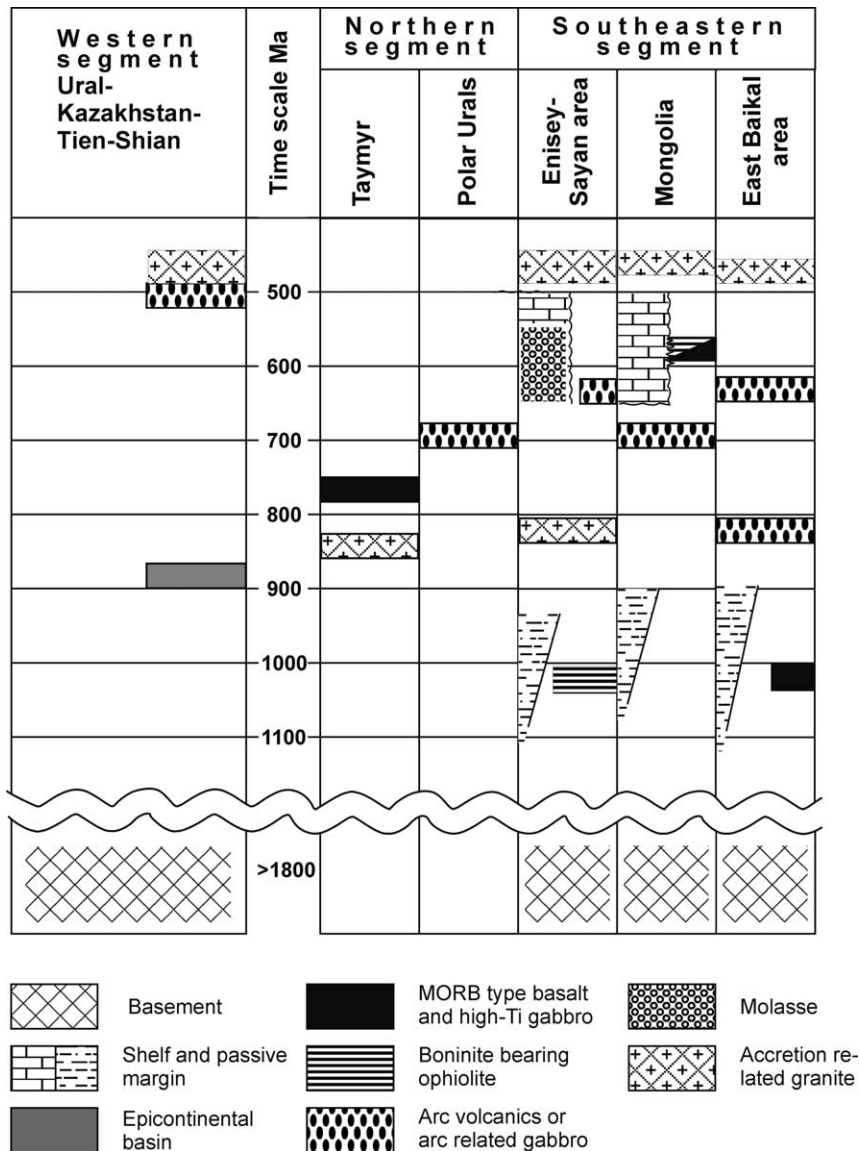

Fig. 7. Correlation of major tectonic units and rock assemblages across the Central Asian fold belt.
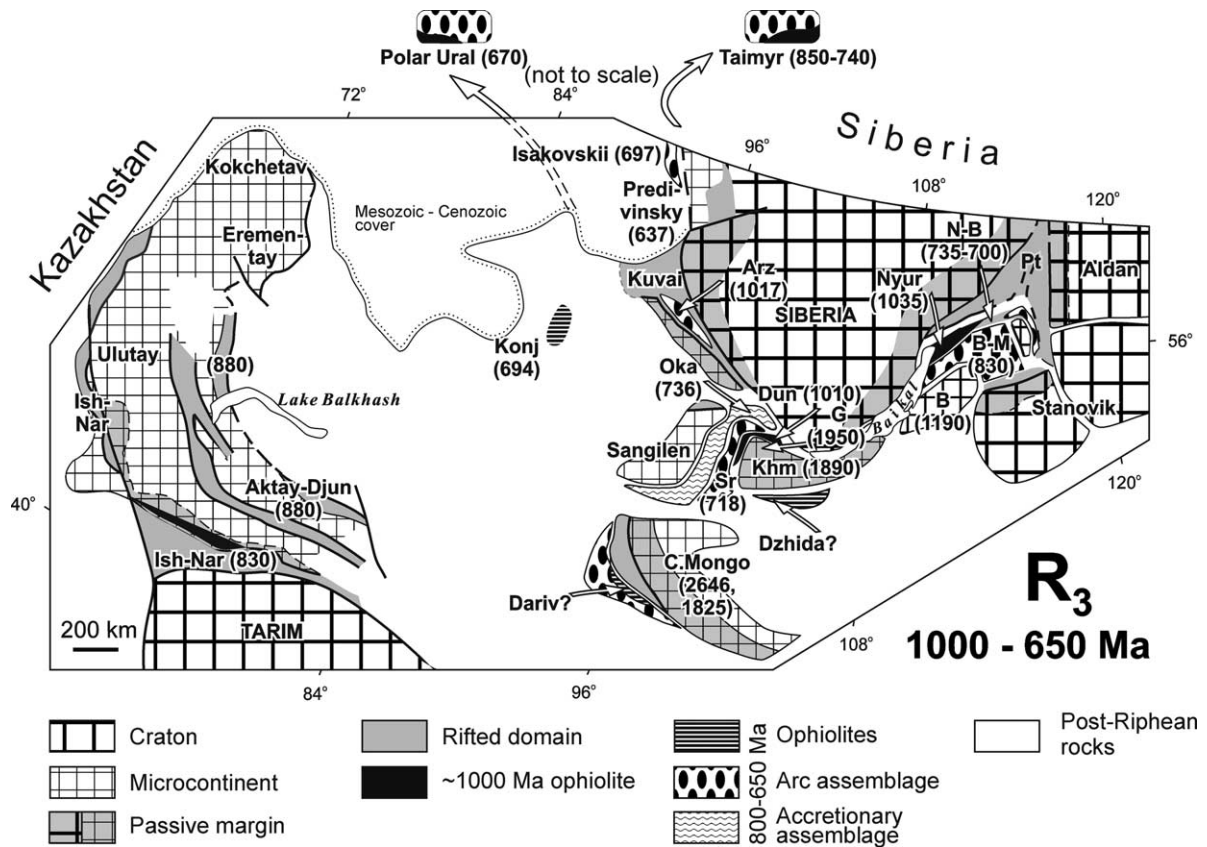
Fig. 8. Main tectonic units and radiometric ages in the southern part of the Central Asian fold belt (present reference frame) during the latest Mesoproterozoic-early Neoproterozoic. For Abbreviations and ages, see Table 3.

in the Enisey Range (Sukhopit, Tungusit and Oslyansk Groups), where land area can be reconstructed in the east (present-day reference frame), whereas farther east there follows a succession of settings from shelf to deep basins with continually migrating shoreline and prograding littoral and basinal facies (Khabarov, 1994). Similar assemblages are documented from the margin of the central Mongolian microcontinent, where clastic–carbonate shelf deposits and turbidites with debris flows, alkaline rift-related basalts, and black shale–carbonate–argillaceous sequences are widespread (Konnikov et al., 1994). Somewhat different assemblages occur on the margins of the Sangilen microcontinent (carbonates of the Derbin and Sangilen Groups) (Gibsher and Terleev, 1992).

During the Neoproterozopicm, the *Kazakhstan–Tarim margin* was dominated by clastic and carbonate–

clastic sequences that unconformably overlie older rocks (Filatova, 1983; Zaitsev, 1984; Brezhnev, 1991; Brezhnev and Raaben, 1992). In northern Kazakhstan (Kokchetav, Ishkeolmes, Erementau–Niyaz, Aktau–Mointin massifs and several massifs in the northern Tien Shan), sandstone–pelite (now quartzite-schist) sequences were laid down (Kokchetav Group and its counterparts). The lower parts of these sequences are made up of schists with sporadic intercalations of marble and quartzite, whereas the upper parts consist of a variety of quartzites and sandstones bearing evidence of their deposition in extremely shallow water (redbeds, cross-bedding, coarse clastics) and contain intercalations that yield rutile–zircon–ilmenite pan samples. The quartzite–schist sequences probably accumulated in a stable epicratonic setting, with a gentle topography in a shallow marine basin (the

schist section) and, then, in a lacustrine alluvial plane (the quartzite section) (Filatova, 1983; Filatova et al., 1988).

In the early Neoproterozoic, on the eastern margin of the Tarim plate and in northern Tien-Shan, rift-related troughs began to develop (Kuruktag, Talass–Karatau, and Kyrgyz–Terskei) that were filled with carbonate–clastic sequences interbedded with stromatolite-bearing limestones, black shales and basalt–rhyolite suites (Brezhnev, 1991; Brezhnev and Raaben, 1992; Abdulin et al., 1986; Mikolaichuk et al., 1997). We suggest that all the sedimentary and volcano–sedimentary assemblages just mentioned formed in epicontinental rift-related basins and on passive margins. The broad distribution of these assemblages on both the Siberian and Kazakhstan–Tarim margins is suggestive of a large basin once separating these margins.

Beginning from about 1100 Ma, an oceanic basin with rift-induced margins began to develop, as in the North Baikal zone, where a passive margin incorporates the Mama–Patom depositional basin and a series of rifts containing within-plate alkali basalts with $\varepsilon_{Nd(t)}$ from −10 to 15. The sedimentary assemblage of the Patom basin erosionally overlies the Mesoproterozoic strata of the Siberian craton, including 2020–2060 Ma granites (U–Pb dating of zircons, Neymark et al., 1998). The base of the sedimentary assemblage is made up of continent-derived highly mature products originating from a basement that had undergone deep chemical weathering as well as from low-K flood basalts as thick as 300 m. These deposits mark the onset of rift-induced extension and possible break-up of the Siberian craton. The early Neoproterozoic age of this event evokes no debate, yet reliable radiometric data are absent.

The earliest record for the existence of oceanic crust begins to appear at about 1000 Ma. Sm–Nd isotopic data for the Nyurundukan suite of the Kicherskaya zone (western segment of the Baykal-Muya belt, Nyur in Fig. 8; Table 3), obtained from four whole-rock metabasalt samples, correspond to an age of 1035±92, $\varepsilon_{Nd(t)} = 7.1$ (Ritsk et al., 1999b). Nd isotope characteristics of siliceous–carbonaceous schists overlying the metabasalts (ε_{Nd} from 5.7 to 4.8, T_{DM} from 1280 to 1020 Ma) suggest a short-lived crustal history and the appearance of oceanic crust (Ritsk et al., 1999b). The first supra-subduction zone complex with an age

of ~1020 Ma is recorded in the Dunzhugur complex of Eastern Sayan (Khain et al., in press, and Section 2.1 above).

A subduction-related complex of the same age was recently identified in the Arzybey complex of the Derbina block (Turkina, 2002) (Fig. 8). The base of the volcanogenic-sedimentary assemblage in this complex is made up of toleiitic metabasalts and a calc-alcalic basalt-andesite-dacite series with REE characteristics suggestive of a subduction setting. Associated with this complexes are tonalites and tronhjemites with typical subduction signatures. A tonalite from this complex yielded a Sm–Nd age (four-point mineral isochron) of 1017 ± 47 Ma, unpublished U–Pb zircon data confirm this age (Turkina, 2002).

Between ~850 and 650 Ma, the margins of the palaeo-ocean became sites of new island-arc systems and back-arc basins (Fig. 7). In the Baikal–Muya volcano-plutonic belt, North Baikal region (B-M in Fig. 8), Izokh et al. (1998) obtained 830–850 Ma Sm–Nd isochron ages for subduction-related gabbros. U–Pb zircon analyses from felsic arc volcanics point to ages of 825±2 and 823±3 Ma, respectively (Ritsk et al., 1999a, 2001). A trondhjemite associated with arc volcanics yielded a U–Pb zircon age of 812±19 Ma (Ritsk et al., 2001). A new phase of subduction-related magmatism in the North Baikal Zone is marked by a belt of layered peridotite-pyroxenite-gabbro massifs with Sm–Nd whole-rock/mineral ages of 735±26 Ma to 704±40 Ma (Amelin et al., 1996) and 630–620 Ma (Amelin et al., 1997; Izokh et al., 1998). In this area, only dismembered fragments of ophiolites are preserved (Dobretsov et al., 1992), and no precise ages are available.

In Taimyr, Vernikovsky (1996) investigated ophiolites as well as tholeiitic and calc-alkaline volcanic arc assemblages that formed at ~740 Ma (Figs. 7 and 8). Similar intra-oceanic associations yielding an age of ~740 Ma also occur in the Enisey Range (Vernikovsky et al., 1999). Along strike of this structure, in the Enganape Range of the Polar Urals, we found ophiolites and related assemblages of evolved intra-oceanic island-arc affinity with an age of ~670 Ma (Khain et al., 1998 and Section 2.4 above; see Figs. 7 and 8).

In East Sayan and northern Mongolia, the Sarkhoi–Darkhat volcanic arc assemblage contains a full spectrum of typical arc volcanics. Felsic volcanic rocks of this arc yielded a Rb/Sr whole-rock age

Table 3
Geochronological data for the main evolutionary stages of the Central Asian fold belt

Ref. no.	Zone	Object of study	Index in Figs. 8–10	Rock type	Analyzed material	Age (Ma)	Isotopic system	Reference
Basement of Siberian margin and/or terranes accreted to Siberian margin								
1	Margin of Khamardaban block, Darib–Shishkhid–Gargan belt	Core of Gargan antiform	G	Gneiss-granite basement	Granite-gneiss, WR	2905 ± 170	Pb–Pb	Neymark et al. (1995)
2	Basement of Central Mongolian block	Baidarik complex	C. Mongol.	Tonalitic gneiss	Zircon	2646 ± 45	U–Pb	Kozakov et al. (1993)
3	Basement of Central Mongolian block	Baidarik complex	C. Mongol.	Tonalitic gneiss	Zircon	2650 ± 30	U–Pb	Mitrofanov et al. (1985)
4	Margin Khamardaban block, Darib–Shishkhid–Gargan belt	Gargan antiform, core of Daban-Zhalga dome	G	Trondhjemitic gneiss	Zircon	ca. 2160	U–Pb	Khain et al. (1995b)
5	Darib–Shishkhid–Gargan belt	Gargan antiform, core of Daban-Zhalga dome	G	Trondhjemitic gneiss	Zircon	1950 ± 10	U–Pb	Khain et al. (1995b)
6	Sarminskii belt (Baikal-Patom basement-?)	Granulites of Cape Kaltygey	Pt	Garnet-cordierite-sillimanite granulite	Zircon	1880	U–Pb	Bibikova et al. (1987)
7	Priolkhon'e: Khamardan (?) basement	Granite-gneiss dome	Khm	Granite-gneiss	Zircon	1890 ± 25	U–Pb	Bibikova et al. (1990)
8	Basement of Central Mongolian block	Baidarik complex	C. Mongol.	Amphibolite	Zircon	1825 ± 5	U–Pb	Kotov et al. (1995)
9	Barguzin block	Barguzin complex, AngaroVitim batholith	B	Granite	Zircon	1190 ± 60	U–Pb	Neymark et al. (1993)
1000–650 Ma Tarim–Kazakhstan margin								
10	Aktay-Djungar	Altynsyngan suite	Aktay-Djun	Rift-related (?) felsic rocks (porphyroid & gneiss)	Zircon	880 ± 11	U–Pb	Khalilov et al. (1993)
11	Ishim-Narun	Bolshoy Naryn suite	Ish-Nar	Rift-related (?) felsic volcanics	Zircon	830 ± 30	U–Pb	Kiselev et al. (1993)
12	Southern Kazakhstan	Koyandisani-Usynbulak area		Rift-related felsic volcanics	Zircon	820–775	Pb–Pb	Gruschka et al. (1999)
Siberian margin								
13	Baikal-Muya belt, West (North Baikal) segment	Nyurundukan unit	Nyur	Metabasalt (MORB-type)	WR-Garnet WR, n = 6	1050 ± 160	Sm–Nd	Neymark et al. (1991)
						1035 ± 92	Sm–Nd	Ritsk et al. (1999b)
14	Arzybey block	Bol'shearzybey massif	Arz	Tonalite-trondhjemite arc related complex	Hb, Pl, Ap, WR	1017 ± 47	Sm–Nd	Turkina (2002)
15	Darib–Shishkhid–Gargan belt	Dunzhugur ophiolite	Dun Plagiogranite	Zircon 1010 ± 10		1019.9 ± 0.7	U–Pb conv.	Khain et al. (in press)
							Pb–Pb evaporation	
16	Faddey zone, Taimyr	Zhdanov massif	Taimyr	Syncollisional (?) granites	Zircon	846 ± 11	U–Pb	Vernikovsky et al. (1998)
					Zircon	840	Th–U–Pb	Pease and Vernikovsky (2000)
17	Baikal-Muya belt, East (Muya) segment	Marinkinskii massif	B-M	Leicocratic gabbro, suprasubduction affinity	Ap, Pl, CPx, WR	835 ± 12	Sm–Nd	Izokh et al. (1998)
18	Baikal-Muya belt, West (North Baikal) segment	Pravomamskaya zone	B-M	Felsic arc volcanics	Zircon	825 ± 3	U–Pb	Ritsk et al. (1999a)
19	Baikal-Muya belt, East (Muya) segment	Kelyano-Irokindiskaya zone	B-M	Felsic arc (?) volcanics	Zircon	824 ± 2	U–Pb	Ritsk et al. (2001)

20	Baikal-Muya belt, West (North Baikal) segment	Kicherskaya zone	B-M	Granite-gneiss-(sinmetamorphic)	Zircon	815 ± 46	U–Pb	Ritsk et al. (1999a)
21	Baikal-Muya belt, East (Muya) segment	Kelyano-Irokindiskaya zone	B-M	Plagiogranite associated with felsic arc (?) volcanics	Zircon	812 ± 19	U–Pb	Ritsk et al. (2001)
22	Darib–Shishkhid–Gargan belt	Gargan massif in Gargan dome, core of antiform	G	Syncollisional (?) tonalite	Hbl, Bi, WR	812 ± 18	Rb–Sr	Kuzmichev et al. (2001)
					Pl, Amf, Bi, WR	800 ± 19	Rb–Sr	
					Zircon	785 ± 11	U–Pb	
23	Baikal-Muya belt, East (Muya) segment	South Muya metamorphic block	B-M	Granite-gneiss-(sinmetamorphic)	Zircon	786 ± 9	U–Pb	Ritsk et al. (2001)
24	Baikal-Muya belt, East (Muya) segment	North Muya metamorphic block	B-M	Granite gneiss-(sinmetamorphic)	Zircon	784 ± 6	U–Pb	Ritsk et al. (2001)
25	Cheliuskin belt, Taimyr	Granite massif	Taimyr	Tonalite	Zircon	740 ± 38	U–Pb	Vernikovsky (1996)
26	Darib–Shishkhid–Gargan belt boundary (Oka) zone	Pyroxenite-gabbro sill in Oka unit	Oka	Gabbro-diabase	Ap, Pl, CPx, WR	736 ± 43	Sm–Nd	Kuzmichev and Zhuravlev (1999)
27	Baikal-Muya belt, East (Muya) segment	Kedrovskii massif	B-M	High-Ti gabbro	Pl, Px, WR	735 ± 26	Sm–Nd	Ritsk et al. (2001)
28	Baikal-Muya belt, East (Muya) segment	Irokindinskii massif	B-M	High-Ti gabbro		733 ± 40	Rb–Sr	Konnikov et al. (1999)
29	Darib–Shishkhid–Gargan belt	Sarkhoy unit	Sr	Arc volcanics	WR, n = 7	718 ± 30	Rb–Sr	Buyakaite et al. (1989)
30	Synnyr zone Baikal-Muya (West)—Baikal-Patom boundary	Dovyren massif	B-M/Pt	Gabbro-norite sill below bottom of Dovyren intrusion	Pl, Bt, WR, OPx, CPx	707 ± 40	Sm–Nd	Amelin et al. (1996)
31	Baikal-Muya belt, East (Muya) segment	Srednemama-kanskii massif	B-M	Gabbro-norite	OPx, CPx, Pl WR (n = 4)	704 ± 71	Sm–Nd	Ritsk et al. (2001)
				Clinopyroxenites and gabbroides from layered anortosite-gabbro massif		774 ± 67	Sm–Nd	
32	Yenisei Range	Porozhinskii massif	Poro-zhinskii	Low-alkaline granite	Zircon	697 ± 4	U–Pb	Vernikovsky et al. (2001)
33	Tom' block, Kuznetskii Alatay Range	Konjinsky unit	Konj	N-MORB basalts	Pl, Amf, WR	694 ± 43	Sm–Nd	Vladimirov et al. (1999)
34	Synnyr zone Baikal-Muya (West)—Baikal-Patom boundary	Dovyren massif	B-M/Pt	Olivine gabbro from the layered series of the mafic-ultramafic supra-subduction (?) intrusion	Pl, CPx, WR	673 ± 22	Sm–Nd	Amelin et al. (1996)
35	Enganepe Range, Polar Urals	Ophiolite assemblage	Polar Urals	Plagiogranite	Zircon	670 ± 5	U–Pb	Khain et al. (1998), this study
36	Baikal-Muya belt, East (Muya) segment	Karalon-Mamakanskaya zone	B-M	Felsic arc volcanics	Zircon	664 ± 3	U–Pb	Ritsk et al. (2001)
37	Baikal-Muya belt, East (Muya) segment	North Muya metamorphic block	B-M	Eclogite	Gr, Px, WR	653 ± 21	Sm–Nd	Shatskii et al. (1996)
38	Baikal-Muya belt, West (North Baikal) segment	plagiogranite, and plagiomigmatite in Nyurundukan suite	B-M	Plagiogranite	Zircon	550–658	U–Pb	Neymark et al. (1995)

Siberian margin, 650–520 Ma

39	Yenisei Range	Predivinsky complex	Pr	Felsic arc volcanic	Zircon	637 ± 6	U–Pb	Vernikovsky et al. (1999)

Table 3 (*Continued*)

Ref. no.	Zone	Object of study	Index in Figs. 8–10	Rock type	Analyzed material	Age (Ma)	Isotopic system	Reference
40	Baikal-Muya belt, West (North Baikal) segment	Chaya massif	B-M	Mantle tectonites	Minerals from harzburgite (2 samples)	640 ± 58	Sm–Nd isochron	Amelin et al. (1997)
				Supra-subduction (?) mafic complex	Minerals from mafic rocks (4 samples)	620 ± 71	Pb–Pb WR isochron	
						627 ± 25	Sm–Nd isochron	
41	Baikal-Muya belt, West (North Baikal) segment	Slyudinskii massif	B-M	High-Ti gabbro-norite	Pl, OPx, CPx, WR	618 ± 61	Sm–Nd	Makrygina et al. (1993)
42	Baikal-Muya belt, West (North Baikal) segment	Nyurundyukan unit	B-M	Enderbite of granulite complex	Zircon	617 ± 5	U–Pb	Amelin et al. (2000)
43	Baikal-Muya belt, East (Muya) segment	Zaoblachnyi massif	B-M	Supra-subduction gabbro	Gabbro-norite (2 samples), Ap, Pl, Cpx, WR	612 ± 62	Sm–Nd	Izokh et al. (1998)
44	Baikal-Muya belt, West (North Baikal) segment	Tonkii mys massif	B-M	High-Mg gabbro	Pl, Ol, CPx, WR	585 ± 22	Sm–Nd	Makrygina et al. (1993)
45	Polar Urals	Dzela metamorphic complex		Metadiorite	Zircon	578 ± 8	Th–U–Pb	Remizov and Pease (in press)
46	Priolkhon'e: Baikal-Muya—Khamardaban boundary (?)	Krestovskii massif	B-M/Khm	Gabbro, diorites, granites	WR	570 ± 18	Rb–Sr	Makrygina et al. (1999)
47	ATCO	Agardag ophiolite	Ag	Plagiogranite	Zircon	570 ± 1	U–Pb	Pfänder et al. (1998), Pfänder and Kröner (in press)
48	Darib–Shishkhid–Gargan belt	Bayannur ophiolite (Dariv Range)	Dariv	Plagiogranite	Zircon	573 ± 6	U–Pb	Khain et al. (1999a,b), this study
49	Darib–Shishkhid–Gargan belt	Khan-Taishir ophiolite	Khantaishir	Plagiogranite	Zircon	568 ± 4	U–Pb	Khain et al. (1999a), Gibsher et al. (2001)
50	Bayan-Khongor zone	Bayan-Khongor ophiolite	Bayan-Khongor	Gabbro	Minerals	569 ± 21	Sm–Nd	Kepezhinskas et al. (1991)
51	Tom' "block", Kuznetsky Alatay Range	Koltass suite	Kz	Felsic volcanic associated with tholeiitic basalt	Zircon	544 ± 8	U–Pb	Vladimirov et al. (1999)
52	Sangilen (block-?)	Moren metamorphic Comlpex	Sangilen	Veins of anatectic (?) tonalite	Zircon	536 ± 6	U–Pb	Kozakov et al. (1999), Salnikova et al. (2001)
53	Lake zone	Bayan-Tsagan massif, Khirgisnur Complex	Lake zone	Supra-subduction gabbro	Pl, 2 Px fractions	531 ± 27	Sm–Nd	Khain et al. (1995a)
54	Priolkhon'e: Baikal-Muya–Khamardaban boundary (?)	Birkhin massif	B-M/Khm	Subalkaline gabbro	Di, Ap, WR	530 ± 23	Sm–Nd	Bibikova et al. (1990)
55	Lake zone	Volcanogenic-sedimentary sequence	Lake zone	Layered gabbro from sill, basalt	CPx, WR	527 ± 43	Sm–Nd	Kovalenko et al. (1996)
56	Lake zone	Volcanogenic-sedimentary sequence	Lake zone	Basalt	Ol, WR, CPx, Amf	522 ± 13	Sm–Nd	Kovalenko et al. (1996)
Siberian margin, 510–450 Ma								
57	Darib–Shishkhid–Gargan belt	Metamorphic complex, Dariv Range	Dariv	Garnet-hypersthene granulite	Zircon	499 ± 3	U–Pb	Kozakov et al. (2002)
58	Derbinskaya zone	Derbina	Derbina	Dunite-pyroxenite-gabbro complex		490		Izokh (personal communication)
59	Sangilen (block-?)	Bayangol magmatic association in Erzin metamorphic complex	Sangilen	Orthopyroxene diorite	Zircon	497 ± 3	U–Pb	Salnikova et al. (2001)

60	Sangilen (block-?)	Dyke in Erzin metamorphic complex	Sangilen	Garnet-hypersthene dyke	Zircon	494 ± 11	U–Pb	Salnikova et al. (2001)
61	Darib–Shishkhid–Gargan belt	Tonalite in metamorphic complex, Dariv Range	Dariv	Biotite-hornblende tonalite	Zircon	490 ± 4	U–Pb	Kozakov et al. (in press)
62	Sangilen (block-?)	Chzhargalan pluton in Naryn metamorphic complex	Sangilen	Granosyenite	Zircon	490 ± 3	U–Pb	Salnikova et al. (2001)
63	Khamardaban block	Veins in Slyudyanskiy Complex	Khamardaban	Hypersthene biotite trondhjemite	Zircon Zircon	488.5 ± 0.6 481 ± 5	U–Pb U–Pb	Salnikova et al. (1998), Kotov et al. (1997)
64	Khamardaban block	Slyudyanskiy Complex	Khamardaban	Two-pyroxene trondhjemite	Zircon	488 ± 0.5	U–Pb	Salnikova et al. (1998)
65	Lake zone	Khovd metamorphic complex	Lake zone	Crystalline schist	Gr, Pl, Bi, WR	487 ± 6	Sm–Nd	Kovalenko et al. (1996)
66	Olkhon island, West Baikal: Baikal-Muya—Khamardaban boundary	Olkhon unit	Olkhon	Granulite	Zircon	485 ± 5	U–Pb	Bibikova et al. (1990)
67	Sangilen (block-?)	Teskhem pluton in Erzin metamorphic complex	Sangilen	Granosyenite	Zircon	480 ± 5	U–Pb	Salnikova et al. (2001)
68	Khamardaban block	Slyudyanskiy complex	Khamardaban	Two-pyroxene trondhjemite	Zircon	477 ± 2	U–Pb	Salnikova et al. (1998)
69	Khamardaban block	Malobystrinskii massif, dyke-type apophysis	Khamardaban	Amphibole-two-pyroxene quartz syenite post-metamorphic	Zircon Zircon	474 ± 5 471 ± 2	U–Pb U–Pb	Kotov et al. (1997), Salnikova et al. (1998)
70	Darib–Shishkhid–Gargan belt	Gargan antiform, core of Daban-Zhalga dome	Gargan	Biotite plagiogneiss and porphyry granites	Zircon, shpene	450–480	U–Pb	Khain et al. (1995b)
71	Khamardaban block	Granite-pegmatite massif in Kultuk suite	Khamardaban	Alaskite granite-pegmatite	Zircon	477 ± 5	U–Pb	Reznitskii et al. (2000)
72	Sangilen (block-?)	Bayangol massif	Sangilen	Granites, quartz diorite	WR	476 ± 8	Rb–Sr	Petrova and Kostitsyn (1997), Petrova (2001)
73	Sangilen (block-?)	West Sangilen	Sangilen	Migmatite	Pl, Mu	474 ± 3	Rb–Sr	Petrova (2001)
74	Sangilen (block-?)	Bashkimygyr pluton in Moren meta morphic complex	Sangilen	Orthopyroxene quartz diorite Quartz diorite	Zircon WR	465 ± 6 464 ± 5	U–Pb Rb–Sr	Salnikova et al. (2001) Petrova (2001)
75	Darib–Shishkhid–Gargan zone, Dariv Range	Differentiated sill of Dariv intrusive complex	Dariv	Amph gabbro	Pl, Ap, Phl, Amph, WR	457 ± 40	Sm–Nd	Khain et al. (1995a)
76	Framing of Sangilen (block-?)	Tannuola Complex in East Tannuola zone	Sangilen	Gneissose quartz diorites	Zircon	457 ± 3	U–Pb	Kozakov et al. (2001)
77	Framing of Sangilen (block-?)	Tannuola Complex in Kaakhem zone	Sangilen	Gneissose quartz diorite	Zircon	451 ± 6	U–Pb	Kozakov et al. (1998)
78	Framing of Sangilen (block-?)	Tannuola Complex in East Tannuola zone	Sangilen	Gneissic diorite	Zircon	512.1 ± 1.0	Pb–Pb evaporation	Kröner and Pfänder (unpublished data)
79	Framing of Sangilen (block-?)	Tannuola Complex in East Tannuola zone	Sangilen	Metagabbro	Zircon	446.7 ± 1.1	Pb–Pb evaporation	Kröner and Pfänder (unpublished data)
80	Baikal-Muya belt, East (Muya) segment	South Muya metamorphic block		Granite-gneiss-	Zircon	445 ± 49	U–Pb	Ritsk et al. (2001)

Data for western Tarim–Kazakstan part of the fold belt (the Tarim–Kazakstan margin of the Palaeo-Asian ocean) and the eastern Siberian margin are listed separately. Complexes referred are shown in Figs. 8–10.

of ~720 Ma (Buyakaite et al., 1989). Compositionally more differentiated volcanic series extend farther into western Mongolia, where they are represented by the Dariv-Ulanshandin volcanic arc (Konnikov et al., 1994; Fig. 8).

Throughout the early Neoproterozoic the *Tarim–Kazakhstan margin* remained passive, and rift-related settings have been reconstructed. For example, felsic volcanic rocks probably associated with a rifting event SW of Lake Balkash provided zircon ages of ~775–820 Ma, and a Nd_{DM} model age of 1.87 Ga, suggest remelting of mid-Proterozoic crust (Gruschka et al., 1997). Therefore, over a long time span between ~1000 and 650 Ma, the PAO was a large asymmetrical structure with a complex active margin on the east and a passive margin on the west (present-day reference frame). At about 800 Ma, in the east accretionary prisms and accretionary magmatism developed (Ritsk et al., 1999a, 2001; Kuzmichev et al., 2001).

3.2. Late Neoproterozoic to earliest Palaeozoic (670–520 Ma)

The next important phase in the history of the PAO was during the time-period 670–520 Ma (Figs. 7 and 9). This phase involved dramatic developments in the PAO. A large island-arc system became extinct, involving closure of related basins, ophiolite obduction and accretion of fragments of these assemblages onto the margins of adjacent continents and microcontinents. All these events were accompanied by the inception of new subduction zones and the opening of new marginal basins. The formation of these assemblages falls into two principal time intervals: 590–570 and 540–520 Ma. The age of the ophiolites in western Mongolia and Tuva as at Bayankhongor (Kepezhinskas et al., 1991), Khantaishir (Khain et al., 1999a; Gibsher et al., 2001, see Section 2.3 above; Fig. 9; Table 3), Dariv (see Section 2.2 above; Fig. 3), and Agardag (Pfänder et al., 1998, in press) is uni-
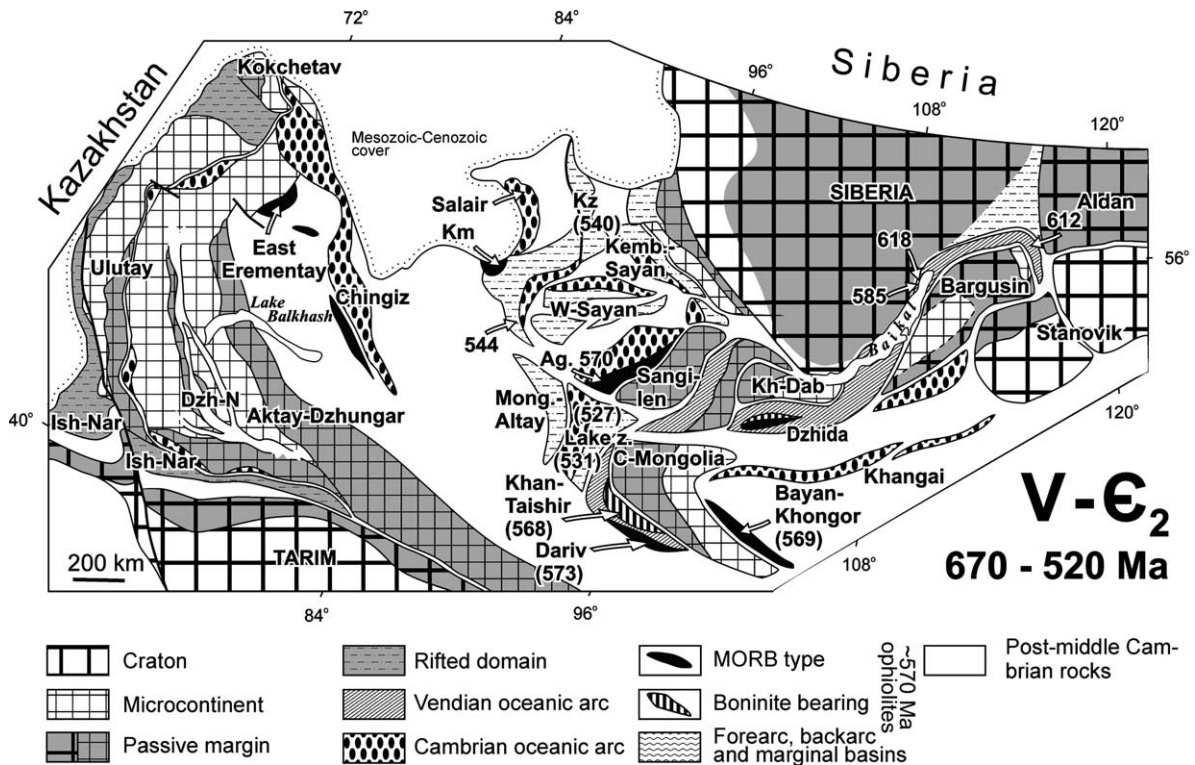

Fig. 9. Main tectonic units and radiometric ages in the southern part of the Central Asian fold belt (present reference frame) during the late Neoproterozoic to middle Cambrian. For Abbreviations and ages, see Table 3.

formly around 570 Ma, using the whole-rock Sm–Nd method and U–Pb and Pb–Pb on zircons (Figs. 7 and 9). At this time, complicated structures along active margins developed, because in ophiolites of this age one can reconstruct tectonic settings of spreading ridges, supra-subduction zones, volcanic arcs and seamounts (e.g., Pfänder et al., in press). In other regions, it was a time of syn-accretionary magmatism and metamorphism, as in the Baikal–Muya folded region to the North (Ritsk et al., 1999a).

In late Neoproterozoic times, the *Kazakhstan–Tarim margin* was still dominated by extension of epicontinental basins, rifted passive margins, and rift-related structures (Fig. 9), whose development began at about 820 Ma ago but continued into the late Neoproterozoic. In the Dzhalair–Naiman zone, continental break-up occurred, sea-floor spreading began, and basins floored by oceanic crust began to form.

In the Ishim–Naryn and Sarytum zones, continental basement provided the site for accumulation of thick, coarse volcano–sedimentary sequences, customarily correlated with diamictites (Zaitsev and Kheraskova, 1979; Kichman et al., 1980; Sagandykov and Sudorgin, 1984), which are usually associated with black shale, sandstone, and siltstone. The volcanic rocks are represented by alkali basalt, trachybasalt, and sporadic basanite and volcaniclastic sediments. These rocks must have formed in a rugged topography in rift-related structures.

During the terminal Proterozoic, eastern Kazakhstan must have represented part of an open marine basin. Fragments of its crust, preserved locally, comprise an assemblage of algal limestones, cherts and MORB-like basalts (Erementau Group) (Ryazantsev et al., 1987).

The most prominent event during the terminal Proterozoic until the middle Cambrian was an extensive transgression that led to passive margin sedimentation on both the Siberian and Kazakhstan–Tarim margins of the PAO, especially on shelves of the continents and microcontinents (Fig. 9). This resulted in extensive carbonate–clastic sequences such as the Tsaganolom Formation of the Dzabkhan zone, central Mongolia; the Canyon Sequence of East Sangilen; the Khubsugul Group of the West Khubsugul area; the Bokson Group of East Sayan and the Baratal Formation of the Mountainous Altay on the Siberian margin. On the Kazakhstan–Tarim margin were deposited the Ka-

pal and Basagin Formations of the Aktau–Dzhungar massif, the Malokaroi Group of the Lesser Karatau, clastic–carbonate sequences on the northern margin of the Tarim continent, and the Volodarsk Formation in the Kokchetav Massif.

At the beginning of the Cambrian, one more structural rearrangement took place in the PAO due to the onset of compression. New island arcs formed, old ones became extinct, remnant arcs converged, and related basins closed.

In the western part of the PAO, systems of volcanic arcs appeared and reached a maximum development (calc-alkaline subduction-related volcanic complexes are found in Kazakhstan, North Tien Shan and, possibly, in the Polar Urals), and this part of the PAO became the site of a system of island arcs, interarc basins and microcontinents. In the eastern part of the ocean, systems of volcanic arcs and microcontinents began to converge with the margin of the Siberian continent, and back-arc and inter-arc basins became gradually closed. During this phase of convergence, new subduction zones were initiated, and volcanic arcs formed.

By mid-Cambrian time, the PAO had become a complex system of oceanic basins, island-arcs, and microcontinents with carbonate–clastic covers. During that time, the architecture of the two parts of the ocean resembled the present-day situation in the western Pacific. The terminal Cambrian until the beginning of the Ordovician was characterized by processes that again had opposite senses in the different parts of the PAO (Fig. 10; Table 3).

3.3. Middle Cambrian and Ordovician (520–450 Ma)

At the end of the Cambrian and in the Ordovician, the western (Tarim–Kazakhstan) margin of the PAO became the site of the strongest pulse of extension, possibly in an environment of shrinking oceans. Numerous basins with oceanic-type crust appeared, as in the Sulu River of SW Kazakhstan where ophiolitic plagiogranite has a zircon age of 510 Ma (Gruschka et al., 1997). Further examples include the Mikain–West Chinghiz (east-central Kazakhstan), the Kyrgyz–Terskei (North Tien Shan) and the Sakmara (West Urals), that varied in life span but all began at the end of the Cambrian to early Ordovician. Simultaneously, the large Turkestan and Uralian basins with oceanic crust began to open.
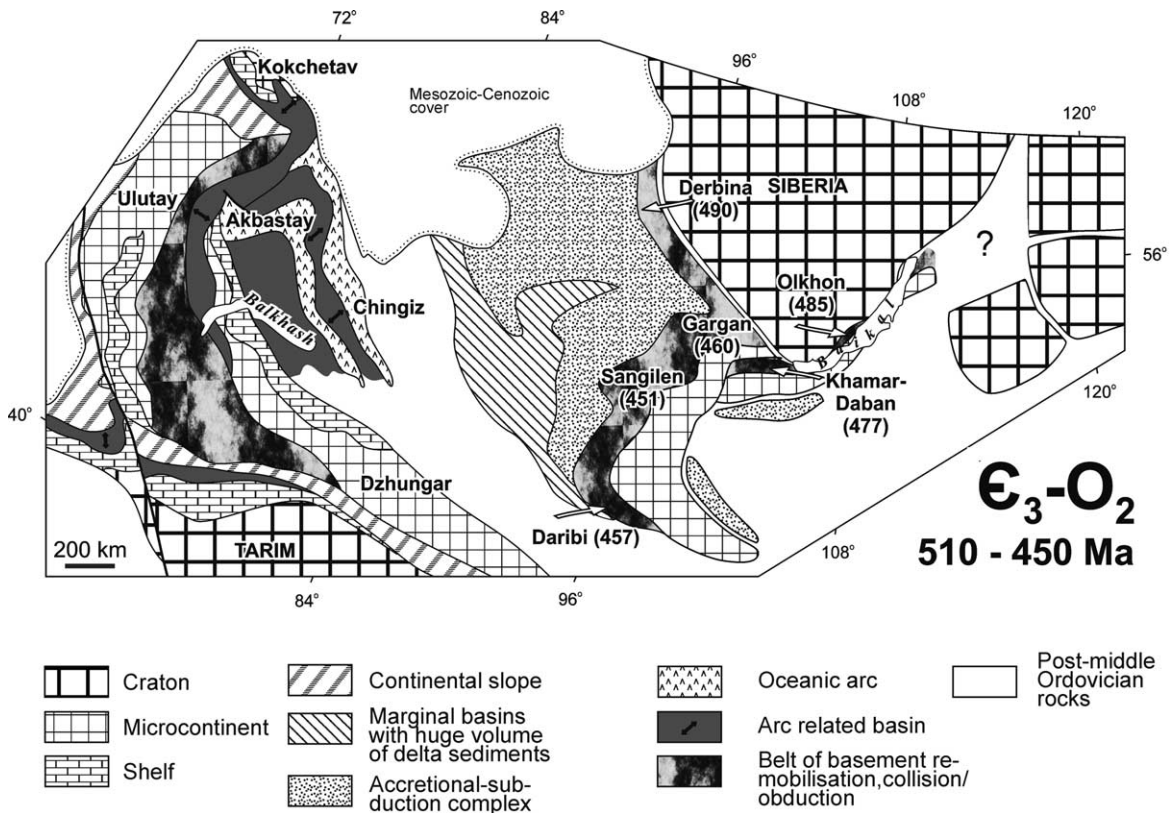
Fig. 10. Main tectonic units and radiometric ages in the southern part of the Central Asian fold belt (present reference frame) during the late Cambrian to middle Ordovician. For Abbreviations and ages, see Table 3.

At the eastern (Siberian–Mongolian) margin of the PAO, this time is marked by collision of island arcs and microcontinents, ridge subduction and closure of interarc basins (Khain, 1989, 1991; Gibsher et al., 1991). This involved the formation of two types of domain:

(1) Subduction–accretion domains (Mountaneous and Mongolian Altai and West Sayan) with crust that incorporates fragments of extinct volcanic arcs and accreted interarc basins. These areas are relatively non-magmatic; thick flysch deposits accumulated in the Mountainous Altai Group and its counterparts during the late Cambrian to Ordovician.

(2) Ridge collision–obduction domains (Tuva, East Sayan, western and northern Mongolia, Trans-Baikalia), where microcontinents are abundant. Here, spreading ridges and volcanic arcs collided with microcontinents and continents,

with accompanying ophiolite obduction, vigorous crustal and crust–mantle magmatism, high-T metamorphism, and strike-slip deformation occurred during the late Cambrian to early Ordovician (Khain, 1989, 1991). Soon after the obduction of ophiolites and related volcanic arcs and closure of marginal basins, the intrusion of mantle-derived mafic-ultramafic rocks took place, granite-gneiss domes emerged, and all rock complexes underwent HT-LP metamorphism up to granulite facies (Kozakov et al., 2002).

Besides these two domains, there remained rather large open basins, which became filled with terrigenous sediments (central and eastern Mongolia) during the late Cambrian to Ordovician (Fig. 10). In late Cambrian to Ordovician times, the western part of the ocean was an active margin of Pacific type, where oceanic basins opened and volcanic arcs

developed. For example, an arc complex near Lake Balkhash in SW Kazakhstan provided zircon ages of 478–480 Ma. These rocks contain zircon xenocrysts as old as 2290 Ma, suggesting remelting of ancient continental crust, and an Andean-type setting is favored (Gruschka et al., 1997).

At the same time, continental masses continued to grow in the eastern part of the PAO, and a peculiar mixed-type margin developed, which had some features in common with accretionary margins (accumulation of thick clastic sequences) and with Andean and Cordilleran margins (intense crust–mantle, ultramafic to gabbroic and granitoid magmatism).

3.4. Palaeogeographic reconstructions

Palaeotectonic schemes (Figs. 8–10) showing the distribution of continental terrains around the PAO and compiled in the present reference frame enable the approximate position of continents, microcontinents and their margins to be reconstructed. The most intriguing issue is the reconstruction for the ~1000–570 Ma time interval, which is critical for the restoration of events that accompanied the growth and break-up of the supercontinent Rodinia. For the period around 1000 Ma, we have used the global palaeogeographic reconstructions of Li et al. (1996) and Pisarevski et al. (in press) (Fig. 11) which show a relatively narrow ocean between Siberia and Laurentia,
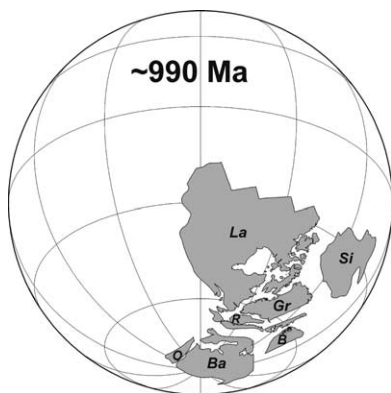

Fig. 11. Palaeogeographic reconstruction of Siberia (Si), Baltica (Ba), Laurentia (La), and neighbouring terranes for 990 Ma on the basis of the best available palaeomagnetic data (modified from Pisarevski et al., in press). Terrane names are as follows: O, Oaxaquia; R, Rockall Plateau; Gr, Greenland; B, Barentsia.

whereas the rest of Siberia is surrounded by an oceanic domain.

Our reconstructions for the Neoproterozoic at 740 and 640 Ma (Figs. 12 and 13), show that a large Palaeo-Asian oceanic basin was located between Baltica, Siberia, Kazakhstan, Tarim and northern China, which were all mutually separated at this time. The existence of this ocean is supported by the development of the Circum-Siberian ophiolite belt (Khain et al., 1997), in which ophiolites and subduction-related magmatic arc complexes became progressively younger (~1000, 800, 650, 570 Ma) from Siberia to the south and west (present-day reference frame). For period 740–640 Ma ago, we have used palaeogeographic reconstructions of (Condie and Rosen, 1994; Torsvik et al., 1995; Pelechaty, 1996; Unrug, 1996; Dalziel, 1997; Weil et al., 1998).

3.4.1. Terminal Mesoproterozoic to early Neoproterozoic, ~990 Ma

In order to decipher the initial stages of inception of the PAO, we have to return to the margins of the supercontinent Rodinia in the late Mesoproterozoic (Fig. 11). The configuration of Rodinia at the end of the Mesoproterozoic at 990 Ma as proposed by Pisarevski et al. (in press) is particularly suitable both geologically and palaeomagnetically. It places the Siberian craton near, but not attached to, the modern northern and northeastern margins of Laurentia.

The configuration of Fig. 11 accounts for the presence of the oldest, ca. 1000 Ma, supra-subduction zone ophiolites and intra-oceanic complexes at Dunzhungur and Nurundukan at the southern and southwestern margins of Siberia (present-day reference frame). We cannot yet compile a detailed reconstruction for this time interval, but the margins of the Siberian craton and the PAO are likely to be still older than the formation of the above complexes (Khain et al., in press). We pointed out previously (Khain et al., 1999a,b, 2001) that the Siberian, Tarim, North China, and Kazakhstan blocks were not, in all likelihood, constituents of the Rodinia supercontinent. Pisarevski et al. (in press), in their global reconstructions, arrived at the same conclusion.

3.4.2. Mid-Neoproterozoic, ~750–670 Ma

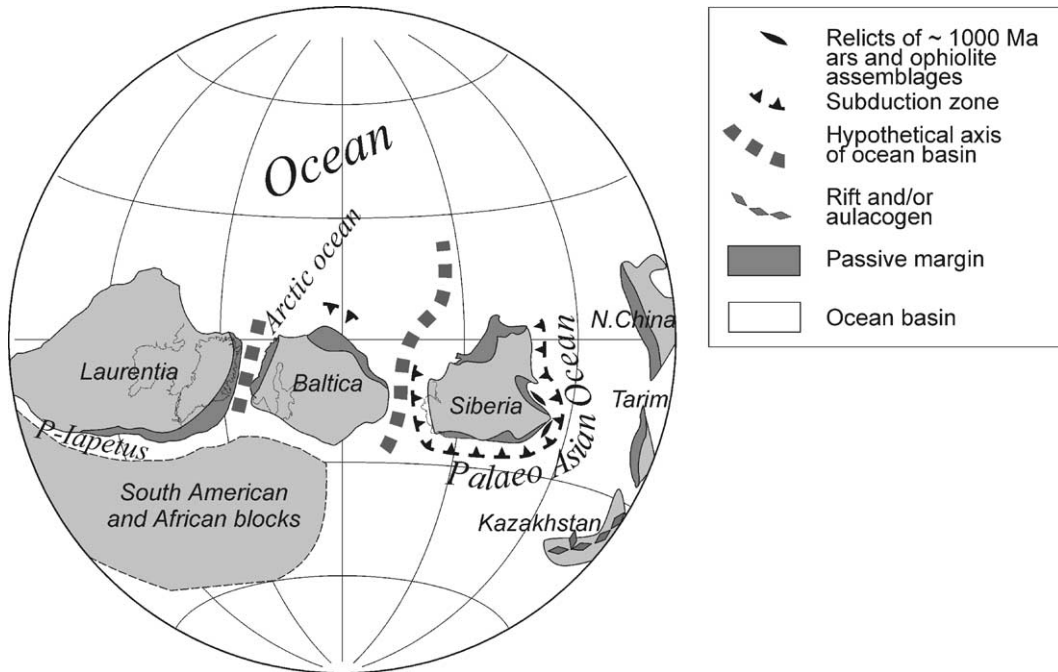Rifting and breakup of Rodinia began not later ~750 Ma, eventually resulting in its complete disper-

Fig. 12. Reconstruction of continents bordering Siberia and the Palaeo-Asian Ocean at ∼740 Ma. All other continents have been omitted.
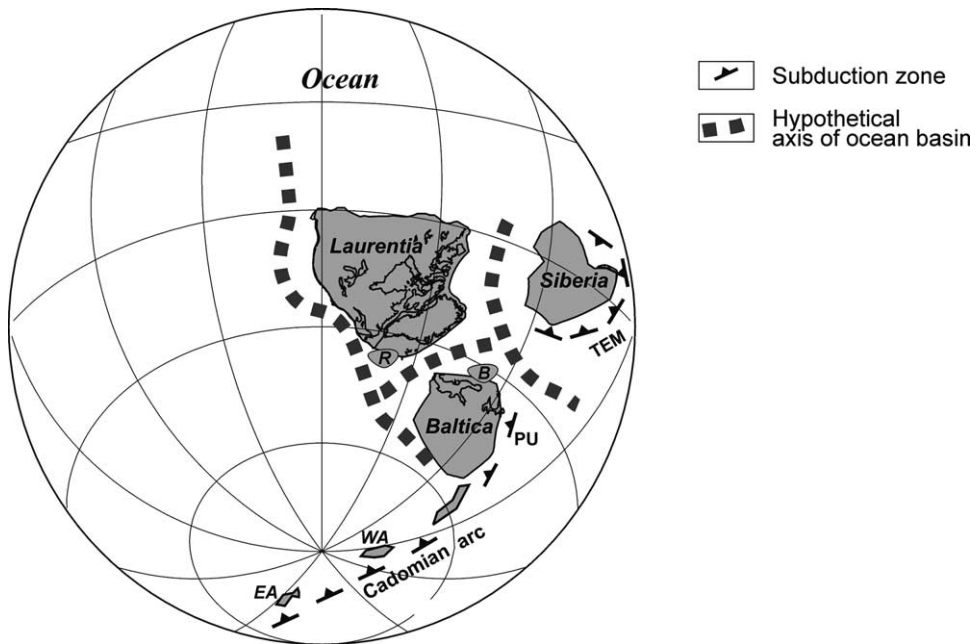

Fig. 13. Reconstruction of continents bordering Siberia and the Palaeo-Asian Ocean at ∼640 Ma. PU, Polar Ural island arc; TEM, Taimyr-Enisei-Mongolian island arc; EA, East Avalonia; WA, West Avalonia; R, Rockall plateau; B, Barentia (Svalbard). All other continents have been omitted. Modified after Dalziel (1997).

sal into several independent continental blocks. Our reconstruction for this time (Fig. 12) only shows the continental masses of Siberia, Baltica and Laurentia as well as the smaller continental terranes of Kazakhstan, Tarim, and Northern China and the oceans separating them. The locations of the North China, Tarim and Kazakhstan continental blocks are shown rather arbitrarily. The latitudinal location and orientation for Tarim have been calculated from Sinian palaeomagnetic poles (Li et al., 1995a,b).

Based on the geological data summarized above, Siberia was most probably detached from Laurentia and Baltica with a small ocean between them, the record of which can still be found in the Polar Urals (Vernikovsky, 1996; this paper). The rifting of Siberia is not limited to its eastern margin, but is also recorded along its western margin, between Laurentia and the blocks of would-be East Gondwana (Li et al., 1996). These blocks will eventually provide a western margin to the PAO basin.

The apparent polar wander path for Siberia reveals insignificant migration in Neoproterozoic times, at a rate of not more than 20–30 km/m.y. (Smethurst et al., 1998; Didenko, unpublished data). This may suggest a relatively fixed position for Siberia and the existence, around this continent, of a long subduction system that impeded its drift. The asymmetric architecture of the continental margins that persisted for a long time, the reiterative emergence and extinction of systems of island arcs and marginal basins, their accretion to continental blocks, the alternating active and passive regimes at the margins, all suggest that, in terms of size and complexity, this palaeo-ocean matched the present-day Pacific Ocean.

3.4.3. Late Neoproterozoic (670–640 Ma)

We now consider the mutual disposal of the main continental blocks adjacent to Siberia and the position of the island arc of the Enganepe massif in the late Neoproterozoic. The equatorial position of Siberia is shown according to the palaeopole (∼650 Ma) of the Ustkurbin redbeds (Pavlov, 1994; Smethurst et al., 1998). It is probable that the Siberian continent was situated in tropical latitudes for a long time interval, for the following reasons:

First, oceanic domains and subduction zone systems already existed at this time around Siberia, and their relicts are represented by ophiolites on the Taimyr, Yeni-

sei and Sayan-Mongolian margins of the Siberian continent (Dergunov, 1989; Didenko et al., 1994; Khain et al., 1997, 1999a). This implies that Siberia, as well as the Mongolian microcontinents, were almost fully surrounded by subduction zones. This subduction zone system substantially lowered the velocity of migration of Siberia and controlled the direction of this migration (east-northeast). Siberia with its late Neoproterozoic margin overrode the Mongolian island arc, moving away from the Arctic margin of Lauretia.

Second, palaeomagnetic data obtained from the Ustkirbinskaya (∼650 Ma) and Ignikanskaya (∼840 Ma) suites (Smethurst et al., 1998) support Siberia's position near the equator, with its Arctic margin turned west-southwest (Fig. 13). It is unlikely that Siberia experienced a substantial drift in the early Neoproterozoic and, by the end of the mid-Neoproterozoic, it returned again to an equatorial latitude. The width of the meridional basin between Siberia and Laurentia is shown conventionally in Fig. 13, but may have been substantially larger.

We can be more specific about the latitudinal position of the Uralian margin of the East European continent (Baltica) and of the Taimyr margin of Siberia in the late Neoproterozoic. If Baltica was situated at no more that $35°$S (Poorter, 1975; Torsvik et al., 1995), and Siberia at about $10°$S, this means that an ocean existed between these two continents with a width of not less than $25°$ (Fig. 13).

3.5. Conclusions

The tentative tectonic reconstructions of Siberia and neighbouring continental terraines as presented above and in Pisarevski et al. (in press) support a long-lived ocean basin around this continent—the Palaeo-Asian ocean. Between ∼1000 and 510 Ma, the PAO probably resembled, in its architecture and evolution, the present-day Indian Ocean with its passive African margin and the complex Australian–Indonesian margin. After 510 Ma, it became structurally similar to the Pacific with its system of volcanic arcs and marginal basins in the west and an Andean–Cordilleran margin in the east.

Using our new age data and published information, it is now possible to approximately restore the principal milestones that mark the appearance of volcanic arcs and marginal basins at about 1100–1000, 830,

740–700, 670–640, 570, 540, and 500–490 Ma, as well as the limits for accretionary and collisional events at about 800, 570, and 470 Ma. All these events occurred in the realm of a major ocean.

The asymmetry of the PAO margins, which persisted for a long period of time, the repeated appearance of volcanic arcs and marginal basin systems, their accretion to continental blocks as well as repeated changes from an active to a passive regime along the continental margins, render this Palaeo-Asian ocean comparable, in terms of size and structural complexity, to the modern Indian and Pacific oceans.

To summarize, precise dating of the Circum-Siberian ophiolites is critical in constraining the evolution of the PAO, which probably came into existence not later than 1100 Ma ago.

Acknowledgements

Appendix A. Analytical techniques for U–Pb multigrain zircon dating

Conventional U–Pb multigrain analyses were undertaken in the Institute of Precambrian Geology and Geochronology (IPGG) in St. Petersburg, using a Finnigan MAT 261 mass-spectrometer in static mode, and in the Vernadsky Intitute of Geochemistry and Analytical Chemistry, Moscow, using a Cameca TSN 206A mass spectrometer.

Zircons were extracted from crushed rock samples using standard heavy liquid and magnetic separation techniques. Hand-picked zircon fractions, consisting of between 20 and 100 grains, were analysed following the method of Krogh (1973). All samples were spiked with a ^{235}U–^{208}Pb mixed tracer. Total blanks were 0.05–0.1 ng Pb and 0.005 ng U. Air-abrasion followed the technique of Krogh (1982), modified by coating the abrasive walls with epoxy-impregnated diamond powder. The PBDAT and ISOPLOT programs of Ludwig (1991a,b) were used for calculating the uncertainties, correlations of U/Pb ratios, regression lines, and concordia intercept ages, and all errors are reported at the 2σ level. The decay constants of Steiger and Jäger (1977) were used for age calculation, and corrections for common Pb were made using the values of Stacey and Kramers (1975).

References

Abdulin, A.A., Kasymov, M.A., Ivlent'ev, I.V., Khaibullin, R.R., 1986. Riphean. Bolshoy Karatau. In: Abdulin, A.A. (Ed.), Geology and Metallogeny of Karatau, vol. 1. Nauka Publ. House, Alma-Ata, pp. 13–15 (in Russian).

Amelin, Y.V., Neymark, L.A., Ritsk, E.Y., Nemchin, A.A., 1996. Enriched Nd–Sr–Pb isotopic signatures in the Dovyren layered intrusion (eastern Siberia, Russia): evidence for source contamination by ancient upper-crustal material. Chemical Geol. 129, 39–69.

Amelin, Y.V., Ritsk, E.Y., Neymark, L.A., 1997. Effects of interaction between ultramafic tectonite and mafic magma on Nd–Pb–Sr isotopic systems in the Neoproterozoic Chaya Massif, Baikal-Muya ophiolite belt. Earth Planet. Sci. Lett. 148, 299–316.

Amelin, Y.V., Rytsk, E.Y., Krymskii, R.S., Neymark, L.A., Skublov, S.G., 2000. Vendian age of enderbites from a granulite complex of the Baikal-Muya ophiolite belt, northern Baikal region: U–Pb and Sm–Nd isotope evidence. Trans. (Dokl.) Russian Acad. Sci. Earth Sci. 371, 455–457.

Berzin, N.A., Coleman, R.G., Dobretsov, N.L., Zonenshain, L.P., Xiao, X.C., Chang, E.Z., 1994. Geodynamic map of the western Palaeoasian ocean. Russian Geol. Geophys. 35, No. 7–8, 8–28.

Bibikova, E.V., Karpenko, S.F., Sumin, L.V., Bogdanovskii, O.G., Kirnozova, T.I., Lialikov, A.V., Makarov, V.A., Arakelyants, M.M., Korikovskii, S.P., Fedorovskii, V.S., Petrova, Z.I., Levitskii, V.I., 1990. In: Shemiakin, V.M. (Ed.), Geology and Geochronology of the Precambrian of the Siberian Platform and Its Framework. Nauka Publ. House, Leningrad, pp. 170–183 (in Russian).

Bibikova, E.V., Korikovsky, S.P., Kirnozova, T.I., Sumin, L.V., Arakelyants, M.M., Fedorovskii, V.S., Petrova, Z.I., 1987. Isotopic-geochronological study of the Baikal-Vitim greenstone belt complexes. In: Shukolyukov, Y.A. (Ed.), Isotopic Studies of Metamorphic and Metasomatic Processes. Nauka Publ. House, Leningrad, pp. 154–164 (in Russian)

Brezhnev, V.D., Raaben, M.E., 1992. Proterozoic deposits of NW and N China: correlation and geodynamic reconstructions. Izvestiya Akad. Nauk. Ser. Geol. 10, 97–110 (in Russian).

Brezhnev, V.D., 1991. Precambrian complexes and some geodynamic features of eastern Tien Shan and North Tarim, Izvestiya Vyzov. Geologiya i Razvedka 2, 3–16 (in Russian).

Buyakaite, M.I., Kuz'michev, A.B., Sokolov, D.D., 1989. 718 Ma Rb–Sr isochron of Sarkhoy Series of Eastern Sayan. Dokl. AN SSSR 309 (1), 150–154 (in Russian).

Condie, K.C., Rosen, O.M., 1994. Laurentia-Siberia connection revised. Geology 22, 168–170.

Dalziel, I.W.D., 1997. Neoproterozoic–Palaeozoic geography and tectonics: review, hypothesis, environmental speculations. Geol. Soc. Am. Bull. 109, 16–42.

Dergunov, A.B., 1989. Caledonides of Central Asia. Nauka Publ. House, Moscow, 192 pp. (in Russian)

Didenko, A.N., Mossakovskii, A.A., Pecherskii, D.M., Ruzhentsev, S.V., Samygin, S.G., Kheraskova, T.N., 1994. Geodynamics of the Central-Asian Palaeozoic oceans. Russian Geol. Geophys. 35, 59–75.

Dobretsov, N.L., Konnikov, E.G., Dobretsov, N.N., 1992. Precambrian ophiolite belts of southern Siberia, Russia, and their metallogeny. Precambrian Res. 58, 427–446.

Dobretsov, N.L., Konnikov, E.G., Medvedev, V.N., Sklyarov, E.V., 1985. Ophiolites and olistostromes of East Sayan. In: Dobretsov, N.L., Zonenshain, L.P., Knipper, A.L., Konnikov, E.G., Sklyarov, E.V. (Eds.), Riphean–Palaeozoic Ophiolites of North Eurasia. Novosibirsk, Nauka Publ. House, pp. 34–58 (in Russian with English abstract).

Dushin, V.A., 1997. Magmatism and Geodynamics of the North Urals Palaeocontinental Sector. Nedra Publ. House, Moscow, 213 pp. (in Russian).

Filatova, L.I., Gvozdik, N.I., Zubatkina, G.M., 1988. On the stratigraphy of the Proterozoic of central Kazakhstan. In: Zaitsev, Y.A. (Ed.), Geology and Minerals of Central Kazakhstan. Nauka Publ. House, Moscow, pp. 15–29 (in Russian).

Filatova, L.I., 1983. Stratigraphy and Historical-Geologic Analysis of the Precambrian Metamorphic Sequences of Central Kazakhstan. Moscow, Nedra, 160 pp. (in Russian).

Gibsher, A.S., Izokh, A.E., Khain, E.V., 1991. Pre-Middle Ordovician structure of Tuva-Mongolian segment of Central Asian fold belt. In: Xiao, X.C., Li, J.Y. (Eds.), Report No. 2 of IGCP Project 283: Geodynamic Evolution and Main Sutures of the Palaeoasian Ocean. Institute of Geology, Chinese Academy of Geological Sciences, Beijing, pp. 25–28.

Gibsher, A.S., Terleev, A.A., 1992. Stratigraphy of the Upper Precambrian and Lower Cambrian of eastern Tuva and northern Mongolia. Russian Geol. Geophys. 38 (11), 26–34.

Gibsher, A.S., Khain, E.V., Kotov, A.B., Salnikova, E.B., Kozakov, I.K., Kovach, V.P., Yakovleva, S.Z., Fedoseenko, A.M., 2001. Late Vendian age of Khan-Taishiri ophiolite complex in Western Mongolia. Russian Geol. Geophys. 42, 1171–1177.

Gruschka, S., Kröner, A., Avdeev, A.V., Seitov, N.S., Oberhänsli, R., 1997. Early Palaeozoic accretion of arcs and microcontinents in the Central Asian Mobile Belt of southern Kazakhstan as deduced from Pb–Pb zircon and Sm–Nd model ages. Terra Nova 9, Abstr.—Suppl. 1, 340.

Izokh, A.E., Gibsher, A.S., Zhuravlev, D.Z., Balykin, P.A., 1998. Sm–Nd data on the age of ultramafic-mafic massifs, eastern branch of the Baikal-Muya ophiolite belt. Dokl. Akad. Nauk. 360 (1), 88–92 (in Russian).

Kepezhinskas, P.K., Kepezhinskas, K.B., Pukhtel, I.S., 1991. Lower Palaeozoic oceanic crust in the Mongolian Caledonides: Sm–Nd isotope and trace element data. Geophys. Res. Lett. 18, 1301–1304.

Khabarov, E.M., 1994. Rock associations and evolution of Riphean sedimentation in the eastern zones of the Yenisei Range. Russian Geol. Geophys. 10, 44–54.

Khain, E.V., 1989. Granite-gneiss domes and ultramafic-mafic intrusions in ophiolite obduction zones. Geotektonika 5, 38–51.

Khain, E.V., 1991. Late Precambrian and early Paleozoic history of the formation of the nappe structure in Eastern Sayan. In: Xiao, X.C., Li, J.Y. (Eds.), Report No. 2 of IGCP Project 283: Geodynamic Evolution and Main Sutures of the Paleoasian Ocean. Institute of Geology, Chinese Academy of Geological Sciences, Beijing, pp. 45–47.

Khain, E.V., Amelin, Y.V., Izokh, A.E., 1995a. Sm–Nd data on the age of ultramafic-mafic complexes in the obduction zone, western Mongolia. Dokl. Akad. Nauk. 341, 791–796 (in Russian).

Khain, E.V., Neymark, L.A., Amelin, Y.V., 1995b. The Caledonian stage of remobilization of the Precambrian basement of the Gargan block, Eastern Sayan (isotopic-geochronological data). Dokl. Akad. Nauk. 342, 776–780 (in Russian).

Khain, E.V., Bibikova, E.V., Dushin, V.A., Fedotova, A.A. 1998. About proposal connection between Palaeo-Asian and Palaeo-Atlantic oceans in Vendian and earle Palaeozic. In: Kariakin, Y.V. (Ed.), Tectonics and geodynamics. Geos Publ. House, Moscow, pp. 244–246 (in Russian).

Khain, E.V., Bibikova, E.V., Degtyarev, K.E., Gibsher, A.S., Didenko, A.N., Klochko, A.A., Rytsk, E.Y., Salnikova, E.B., Fedotova, A.A., 1999a. The Palaeo-Asian ocean in the Neoproterozoic and early Palaeozoic: new radiometric data. In: Kozakov, I.K. (Ed.), Geological History of the Proterozoic Marginal Palaeo-Oceanic Structures of Northern Eurasia. Tema Publ. House, St. Petersburg, pp. 175–181 (in Russian).

Khain, E.V., Gibsher, A.S., Didenko, A.N., Vernikovsky, V.A., Degtyarev, K.E., Fedotova, A.A., 1999b. The Neoproterozoic Palaeo-Asian ocean: age of inception and the Baikalian events. J. Conf. Abstr. 4, No. 1, Terra Abstracts 11, 108 pp.

Khain, E.V., Kröner, A., Gibsher, A.S., Fedotova, A.A., 2001. The fate of Rodinia in the light of the discovery of ca. 1000 Ma old ophiolites in the Central Asian orogenic belt of Siberia. Gondwana Res. 4, 656–658.

Khain, E.V., Bibikova, E.V., Kröner, A., Zhuravlev, D.Z., Sklyarov, E.V., Fedotova, A.A., Kravchenko-Berezhnoy, I.R., in press. The most ancient ophiolite of the Central Asian fold belt: U–Pb and Pb–Pb evidence from the Dunzhugur complex, Eastern Sayan, Siberia, and geodynamic implications. Earth Planet Sci. Lett.

Khain, V.E., Bozhko, N.A, 1988. Historical Geotectonics. Nedra Publ. House, Moscow, 382 pp. (in Russian).

Khain, V.E., Gusev, G.S., Khain, E.V., Vernikovsky, V.A., Volobuyev, M.I., 1997. Circum-Siberian Neoproterozoic ophiolite belt. Ofioliti 22, 195–200.

Khalilov, V.A., Bulina, V.A., Zlobin, G.A., Kim, V.S., 1993. Isotopic age of zircons from crystalline complexes of southern Kazakhstan. In: Rudnik, B.A., Sokolov, Y.M., Filatova, L.I.

(Eds.), Early Precambrian of the Central Asian fold belt. Nauka Publ. House, St. Petersburg, pp. 80–98 (in Russian).

Kheraskova, T.N., Tomutogoo, O., Khain, E.V., 1985. Ophiolites and Upper Precambrian rocks of the Lake Zone, Dariv Ridge (Western Mongolia). Izvestia. Akad. Nauk. SSSR Ser. Geol. 6, 25–31 (in Russian).

Kichman, E.S., Alperovich, E.V., Kovalevskii, A.F., Kozhev, A.V., Nikitchenko, I.I., 1980. Precambrian. In: Abdulin, A.A. (Ed.), Geology of the Chu–Ili Region. Nauka Publ. House, Alma-Ata, pp. 15–33 (in Russian).

Kiselev, V.V., Apayarov, F.K., Komartsev, V.T., Tsyganok, E.N., Lukashova, E.M., 1993. Isotopic age of zircons from crystalline complexes of Tien Shan. In: Rudnik, B.A., Sokolov, Y.M., Filatova, L.I. (Eds.), Early Precambrian of the Central Asian Fold Belt. Nauka Publ. House, St. Petersburg, pp. 99–115 (in Russian).

Konnikov, E.G., Gibsher, A.S., Izokh, A.E., Sklyarov, E.V., Khain, E.V., 1994. Late-Proterozoic evolution of the northern segment of the Paleoasian Ocean: new radiological and geochemical data. Russian Geol. Geophys. 35 (7/8), 152–168.

Konnikov, E.G., Tsygankov, A.A., Vrublevskaya, T.T., 1999. The Baikal-Muya Volcano-plutonic belt: Structures, Substance and Geodynamics. Geos Publ. House, Moscow, 163 pp. (in Russian).

Kotov, A.B., Kozakov, I.K., Bibikova, E.V., Salnikova, E.B., Kirnozova, T.I., Kovach, V.P., 1995. Duration of regional metamorphic episodes in areas of polycyclic endogenic processes: U–Pb geochronological study. Petrology 3 (6), 567–575.

Kotov, A.B., Salnikova, E.B., Reznitskii, L.Z., Vasil'ev, E.P., Kozakov, I.K., Yakovleva, S.Z., Kovach, V.P., Berezhnaya, N.G., 1997. Age of metamorphism of the Slyudyanka crystalline complex, southern Baikal area—U–Pb geochronology of granitoids. Petrology 5 (4), 338–349.

Kovalenko, V.I., Yarmolyuk, V.V., Pukhtel, I.S., Stosch, H., Jagoutz, E., Korikovsky, S.P., 1996. Igneous rocks and magma sources of the Ozernaya zone ophiolites, Mongolia. Petrology 4 (5), 420–459.

Kozakov, I.K., Kotov, A.B., Salnikova, E.B., Bibikova, E.V., Kovach, V.P., Kirnozova, T.I., Berezhnaya, N.G., Lykhin, D.A., 1999. Metamorphic age of crystalline complexes of the Tuva-Mongolia massif: U–Pb geochronology of granitoids. Petrology 7 (2), 177–191.

Kozakov, I.K., Bibikova, E.V., Neymark, L.A., Kirnozova, T.I., 1993. Baidarik block. In: Rudnik, B.A., Sokolov, Y.M., Filatova, L.I. (Eds.), Early Precambrian of the Central Asian Fold Belt. Nauka Publ. House, St. Petersburg, pp. 118–137 (in Russian).

Kozakov, I.K., Kotov, A.B., Salnikova, E.B., Kovach, V.P., Natman, A., Bibikova, E.V., Kirnozova, T.I., Todt, W., Kröner, A., Yakovleva, S.Z., Lebedev, V.I., Sugorakova, A.M., 2001. Timing of the structural evolution of metamorphic rocks in the Tuva-Mongolian massif. Geotectonics 35, 165–184.

Kozakov, I.K., Salnikova, E.B., Khain, E.V., Kovach, V.P., Berezhnaya, N.G., Yakovleva, N.G., Plotkina, Yu.V., 2002. Early Caledonian crystalline rocks of the Lake zone, Mongolia: Stages and tectonic environments as deduced from U–Pb and Sm–Nd isotopic data. Geotectonics 36, 156–166.

Kozakov, I.K., Salnikova, E.B., Kovalenko, V.I., Kotov, A.B., Lebedev, V.I., Sugorakova, A.M., Yakovleva, S.Z., 1998. The

age of postcollision magmatism of early Caledonides of Central Asia, with the Tuva region as an example. Trans. (Dokl.) Russian Acad. Sci. Earth Sci. 360, 510–513.

Krogh, T., 1973. A low contamination method for hydrothermal decomposition of zircons and extraction of U and Pb for isotope determinations. Geochim. Cosmochim. Acta 37, 485–495.

Krogh, T., 1982. Improved accuracy of U–Pb zircon by the creation of more concordant systems using an air abrasion technique. Geochim. Cosmochim. Acta 46, 637–649.

Kuzmichev, A.B., Bibikova, E.V., Zhuravlev, D.Z., 2001. Neoproterozoic (800 Ma) orogeny in the Tuva-Mongolian Massif (Siberia): island arc-continent collision at the northeast Rodinia margin. Precambrian Res. 110, 109–126.

Kuzmichev, A.B., Zhuravlev, D.Z., 1999. Pre-Vendian age of the Oka Group, Eastern Sayan: evidence from Sm–Nd dating of sills. Trans. (Dokl.) Russian Acad. Sci. Earth Sci. 365 (2), 173–177.

Li, J., Li, Q., Zhang, H., Sun, D., Cao, J., Wu, S., 1995a. Palaeomagnetic study of Tarim and its adjacent area as well as the formation and evolution of Tarim basin. Xinjiang Geol. 13, 293–377.

Li, Z.X., Zhang, L., Powell, C.McA., 1995b. South China in Rodinia: part of the missing link between Australia-East Antarctica and Laurentia? Geology 23, 407–410.

Li, Z.X., Zhang, L., Powell, C.McA., 1996. Positions of the East Asian cratons in the Neoproterozoic supercontinent Rodinia. Aust. J. Earth Sci. 43, 593–604.

Ludwig, K.R., 1991a. ISOPLOT program. US Geol. Surv. Open File Report 91, 35 pp.

Ludwig, K.R., 1991b. PbDat for MS-DOS, version 1.21. US Geol. Surv. Open-File Report 91, 35 pp.

Makrygina, V.A., Konnikov, E.G., Neymark, L.A., Pakhol'chenko, Y.A., Posokhov, V.F., Sandimirova, G.P., Tomilenko, A.A., Tsygankov, A.A., Vrublevskaya, T.T., 1993. The age of granulite-charnockite complex of Nurundyukan Suite, northern Cisbaikalia (paradox of radiochronology). Dokl. Acad. Nauk. 332, 486–490 (in Russian).

Makrygina, V.A., Petrova, Z.I., Sandimirova, G.P., Pakhol'chenko, Y.A., 1999. Confirmation of palaeogeodynamic reconstructions for Priolkhonye: Rb–Sr geochronological data. In: Kozakov, I.K. (Ed.), Geologic Evolution of Proterozoic Marginal Palaeo-Oceanic Structures of Northern Eurasia. Tema Publ. House, St. Petersburg, pp. 70–72 (in Russian).

Mikolaichuk, A.V., Kurenkov, S.A., Degtyarev, K.E., Rubtsov, V.I., 1997. Northern Tien Shan: main stages of geodynamic evolution in the late Precambrian-early Palaeozoic. Geotectonics 31, 445–462.

Mitrofanov, F.P., Bibikova, E.V., Gracheva, T.V., Kozakov, I.K., Sumin, L.V., Shuleshko, I.K., 1985. Archaean isotope age of tonalite ("grey") gneisses within the Caledonian structures of Central Mongolia. Dokl. Acad. Nauk. 284, 670–674 (in Russian).

Mossakovskii, A.A., Ruzhentsev, S.V., Samygin, S.G., Kheraskova, T.N., 1993. Central Asian fold belt: geodynamic evolution and history of formation. Geotectonics 6, 3–33.

Muratov, M.B., 1974. Uralian-Mongolian belt. In: Muratov, M.B. (Ed.), Tectonics of Urals–Mongolian Belts. Nauka Publ. House, Moscow, pp. 5–11 (in Russian).

Neymark, L.A., Rytsk, E.Y., Rizvanova, N.G., 1993. Hercynian age and Precambrian crustal protolith for Barguzinskii granitoids of the Angaro-Vitimskii batholith: U–Pb and Sm–Nd evidence. Dokl. Acad. Nauk. 331, 726–729 (in Russian).

Neymark, L.A., Rytsk, E.Y., Gorokhovsky, B.M., Ovchinnikova, G.V., Kiseleva, E.I., Konkin, V.D., 1991. Lead isotopic composition and genesis of lead-zinc mineralization of the Olokit zone of the northern Baikal region. Geol. Ore Deposits Geologiya rudhykh mestorozhdenii 33 (6), 34–49 (in Russian).

Neymark, L.A., Ritsk, E.Y., Ovchinnikova, G.V., Sergeeva, N.A., Gorokhovsky, B.M., Skopintsev, V.G., 1995. Lead isotopes in gold deposits of Eastern Sayan. Geol. Ore Deposits Geologiya rudhykh mestorozhdenii 37, 237–249 (in Russian).

Neymark, L.A., Larin, A.I., Nemchin, A.A., Ovchinnikova, G.V., Ritsk, E.Y., 1998. Anorogenic nature of magmatism in the northern Baikal volcanic belt: evidence from geochemical, geochronological (U–Pb), and isotopic (Pb, Nd) data. Petrology 6 (2), 124–148.

Pavlov, V.E., 1994. Palaeomagnetic poles for the Uchur–Maya hypostratotype of the Riphean: riphean drift of the Aldan Block of the Siberian craton. Dokl. Akad. Nauk. 336, 533–537.

Pease, V., Vernikovsky, V., 2000. The tectonic-magmatic evolution of the Taimyr Peninsula: further constraints from new ion-microprobe data. Polarforschung 68, 1–3.

Pelechaty, S.M., 1996. Stratigraphic evidence for the Siberia-Laurentia connection and early Cambrian rifting. Geology 24, 719–722.

Petrova, A.Y., Kostitsyn, Y.A., 1997. Age of high-grade metamorphism and granite magmatism in western Sangilen. Geochem. Int. (Geokhimiya) 35 (3), 295–298.

Petrova, A.Y., 2001. Rb–Sr isotope system in metamorphic and magmatic rocks of western Sangilen (south-eastern Tuva). Unpubl. Can. Sci. (Geol. Mineral.) Dissertation. Institute of Mineralogy, Geochemistry and Crystallochemistry of Rare Elements, Russian Academy of Sciences, Moscow, 123 pp. (in Russian).

Pfänder, J.A., Jochum, K.-P., Kozakov, I., Kröner, A., Oidup, C., Todt, W., 1998. Age and geochemical evolution of an early Cambrian ophiolite-island arc system in Tuva, south central Asia. Geol. Surv. Finland Spec. Paper 26, 42.

Pfänder, J.A., Jochum, K.-P., Kozakov, I., Kröner, A., Todt, W., in press. Coupled evolution of back-arc and island arc-like mafic crust in the late Neoproterozoic Agardagh Tes-Chem ophiolite, Central Asia: evidence from trace element and Sr–Nd–Pb isotope data. Contrib. Mineral. Petrol.

Pfänder, J.A., Kröner, A., in press. Tectono-magmatic evolution, age and emplacement of the Agardagh Tes-Chem ophiolite in Tuva, Central Asia: crustal growth by island arc accretion. In: Kusky, T. (Ed.), Precambrian Ophiolites and Related Rocks. Elsevier Science, Amsterdam.

Pisarevski, S.A., Wingate, M.T.D., Powell, C.McA., Johnson, S.P., Evans, D.A.D., in press. Models of Rodinia assembly and fragmentation. In: Yoshida, M., Windley, B.F., Dasgupta, S. (Eds.), Proterozoic East Gondwana: Supercontinent Assembly and Breakup. Geol. Soc. London, Spec. Publ.

Pisarevski, S.A., Natapov, L.M., in press. Siberia and Rodinia. Tectonophysics.

Poorter, R.P.E., 1975. Paleomagnetism of Precambrian rocks from southeast Norway and south Sweden. Phys. Earth Planet. Int. 10, 74–87.

Remizov, D.N., Pease, V., in press. Geochemical and tectonic significance of the Dzela island arc complex. J. Geol. Soc. London.

Reznitskii, L.Z., Kotov, A.B., Salnikova, E.B., Vasil'ev, E.P., Yakovleva, S.Z., Kovach, V.P., Fedoseenko, A.M., 2000. The age and time span of formation of phlogopite and lazurite deposits in the southwestern Baikal Area: U–Pb geochronology. Petrology 8 (1), 66–76.

Ritsk, E.Y., Amelin, Y.V., Krymski, R.S., Rizvanova, N.G., Shalaev, V.S., 1999a. The Baikal–Muya belt: age, formation stages, and crustal evolution (U–Pb and Sm–Nd isotopic evidence). In: Kariakin, Y.V. (Ed.), Tectonics, geodynamics, and the processes of magmatism and metamorphism, vol. 2. Geos Publ. House, Moscow, pp. 93–95 (in Russian).

Ritsk, E.Y., Amelin, Y.V., Krymski, R.S., Shalaev, V.S., Rizvanova, N.G., 1999b. On the age of the Nyurundyukan sequence (Kichera Zone, Baikal–Muya fold belt): New U–Pb and Sm–Nd isotope data. In: Kozakov, I.K. (Ed.), Geologic Evolution of Proterozoic Marginal Palaeo-oceanic Structures of Northern Eurasia. Tema Publ. House, St. Petersburg, pp. 130–132 (in Russian).

Ritsk, E.Y., Amelin, Y.V., Rizvanova, N.G., Krymskii, R.S., Mitrofanov, G.L., Mitrofanova, N.N., Perelyaev, V.I., Shalaev, V.S., 2001. Age of rocks in the Baikal-Muya foldbelt. Stratigraph. Geol. Correlation 9 (4), 315–326.

Ryazantsev, A.V., Herman, L.L., Degtyarev, K.E., Kotlyar, A.L., Fedorov, E.V., 1987. Lower Palaeozoic chaotic complexes in eastern Erementau (central Kazakhstan). Dokl. Akad. Nauk. SSSR 296, 320–324 (in Russian).

Sagandykov, K.S., Sudorgin, A.A., 1984. Dzhetym Iron-Bearing Basin of Tien Shan. Ilim Publ. House, Frunze, 216 pp. (in Russian).

Salnikova, E.B., Sergeev, S.A., Kotov, A.B., Yakovleva, S.Z., Steiger, R.H., Reznitskiy, L.Z., Vasil'ev, E.P., 1998. U–Pb zircon dating of granulite metamorphism in the Sludyanskiy complex, eastern Siberia. Gondwana Res. 1, 195–205.

Salnikova, E.B., Kozakov, I.K., Kotov, A.B., Kröner, A., Todt, W., Bibikova, E.V., Nutman, A., Yakovleva, S.Z., Kovach, V.P., 2001. Age of Palaeozoic granites and metamorphism in the Tuvino-Mongolian Massif of tha Central Asian Mobile belt: loss of a Precambrian microcontinent. Precambrian Res. 110, 143–164.

Scarrow, J.H., Pease, V., Fleutelot, C., Dushin, V., 2001. The late Neoproterozoic Enganepe ophiolite, Polar Urals, Russia: an extension of the Cadomian arc? Precambrian Res. 110, 255–275.

Sengör, A.M.C., Natal'in, B.A., Burtman, V.S., 1993. Evolution of the Altaid tectonic collage and Palaeozoic crustal growth in Eurasia. Nature 364, 299–307.

Sengör, A.M.C., Natal'in, B.A., 1996. Paleotectonics of Asia: fragments of a synthesis. In: Yin, A., Harrison, T.M. (Eds.), The Tectonic Evolution of Asia. Cambridge University Press, Cambridge, UK, pp. 486–640.

Shatskii, V.S., Jagoutz, E., Ryboshlyakov, Y.V., Kozmenko, O.A., Vavilov, M.A., 1996. Eclogites of the North-Muya block—

evidence for Vendian collision in the Baikal-Muya ophiolite belt. Dokl. Akad. Nauk. 350 (5), 677–680 (in Russian).

Sklyarov, E.V., 1988. Riphean—Palaeozoic (?) ophiolite complexes. In: Dobretsov, N.L., Ignatovich, V.I. (Eds.), Geology and Metamorphism of Eastern Sayan. Nauka Publ. House, Novosibirsk, pp. 26–29 (in Russian).

Smethurst, M.A., Khramov, A.N., Torsvik, T.H., 1998. The Neoproterozoic and Palaeozoic palaeomagnetic data for the Siberian platform: from Rodinia to Pangea. Earth Sci. Rev. 43, 1–24.

Sovetov, Y.K., Blagovidov, V.V., 1995. Evolution of the Riphean passive margin of the Siberian continent (Patom Highland). In: Koroteev, V.A. (Ed.), General Problems of the Stratigraphy and Geologic History of the Riphean of Northern Asia. Uralian Branch, Russian Academy of Sciences, Yekaterinburg, pp. 115–116 (in Russian).

Stacey, J.S., Kramers, J.D., 1975. Approximation of terrestrial lead isotope evolution by a two-stage model. Earth Planet. Sci. Lett. 26, 207–221.

Steiger, R.H., Jäger, E., 1977. Subcommission on geochronology: convention on the use of decay constants in geo- and cosmochronology. Earth Planet. Sci. Lett. 36, 803–824.

Tomurtogoo, O., 1989. Ophiolites and formation of folded belts in Mongolia. Unpubl. Doct. (Geol. Mineral.) Dissertation. Geological Institute, Russian Academy of Sciences, Moscow, 300 pp. (in Russian).

Torsvik, T.H., Roberts, D., Siedlecka, A., 1995. Paleomagnetic data from sedimentary rocks and dolerite dykes, Kildin island, Rybachi, Sredni and Varanger Peninsulas, NW Russia and NE Norway: a review. Norsk Geol. Unders., Special Publ, 7, 315–326.

Turkina, O.M., 2002. Tonalite-trondhjemite of subduction-related complexes (Late Riphean plagiogranites) on the SW margin of the Siberian craton. Russian Geol. Geophys. 43, 418–431.

Unrug, R., 1996. The assembly of Gondwanaland. Episodes 19, 11–20.

Vernikovsky, V.A., 1996. Geodynamic Evolution of the Taimyr Folded Area. United Institute of Geology, Geophysics and Mineralogy, Siberian Branch, Russian Academy of Sciences, Novosibirsk, 202 pp. (in Russian with English abstract).

Vernikovsky, V.A., Salnikova, E.B., Kotov, A.B., Kovach, V.P., Yakovleva, S.Z., 1998. Precambrian granites of the Faddey terrane (northern Taimyr): new geochemical and geochronological (U–Pb, Sm–Nd) data. Trans. (Dokl.) Russian Acad. Sci. 363 (9), 1218–1222 (in Russian).

Vernikovsky, V.A., Vernikovskaya, A.E., Sal'nikova, E.B., Kotov, A.B., Chernykh, A.I., Kovach, V.P., Berezhnaya, N.G., Yakovleva, S.Z., 1999. New U–Pb data on the formation of the Predivinsk palaeo-island-arc complex (Yenisey Ridge). Russian Geol. Geophys. 40, 255–259.

Vernikovsky, V.A., Vernikovskaya, A.E., Chernykh, A.I., Salnikova, E.B., Kotov, A.B., Kovach, V.P., Yakovleva, S.Z., Fedoseenko, A.M., 2001. Porozhnaya granitoids of the Enisey ophiolite belt: indicators of the Neoproterozoic events on the Enisey Range. Trans. (Dokl.) Russian Acad. Sci. Earth Sci. 381 (9), 1043–1047.

Vladimirov, A.G., Ponomareva, A.P., Kargopolov, S.A., Babin, G.A., Plotnikov, A.V., Gibsher, A.S., Izokh, A.E., Shokal'skii, S.P., Bibikova, E.V., Zhuravlev, D.Z., Ponomarchuk, V.A., Khalilov, V.A., Travin, A.V., 1999. Neoproterozoic age of the oldest rocks from the Tomsk block (Mountainous Shoriya) according to U–Pb, Sm–Nd, Rb–Sr and Ar–Ar dating. Stratigraph. Geol. Correlation 7 (5), 437–451.

Weil, A., Van der Voo, R., McNiocail, C., Meert, J., 1998. The Proterozoic supercontinent Rodinia: palaeomagnetically derived reconstructions for 1100–800 Ma. Earth Planet. Sci. Lett. 154, 13–24.

Zaitsev, Y.A., Kheraskova, T.N., 1979. The Vendian of Central Kazakhstan. Lomonosov State University, Moscow, 252 pp. (in Russian).

Zaitsev, Y.A., 1984. Evolution of Geosynclines. Nedra Publ. House, Moscow, 208 pp. (in Russian).

Zonenshain, L.P., Kuzmin, M.I., Natapov, L.M., 1990. Geology of the USSR: a plate tectonics synthesis. Am. Geophys. Union Geodyn. Ser. 21, 242.

Zonenshain, L.P., Kuzmin, M.I., 1978. Khantaishir ophiolite complex in western Mongolia and ophiolite problem. Geotektonika 1, 19–42.

Zhuravlev, A.Z., Zhuravlev, D.Z., Kostitsyn, Yu.A., Chernyshov, I.V., 1987. High-precision determination of Sm/Nd ratios from rock samples using isotope dilution. Geokhimia 25, 1115–1129 (in Russian).